

Temporal Trends in Secondary Forest Carbon Sequestration

Jill Derwin

Dr. Jennifer Swenson, Advisor

May 2012

Masters project submitted in partial fulfillment of the
requirements for the Master of Environmental Management degree in

The Nicholas School of the Environment of
Duke University

2012

Table of Contents

Abstract	1
Introduction	2
Objective.....	2
Deforestation and Climate Change.....	3
<i>The role of forest management in Carbon Sequestration</i>	4
Study Area	6
Methods	7
<i>Data Selection</i>	7
<i>Pre-Processing</i>	9
<i>Forest Ageing through Post-Classification Merging</i>	9
<i>Analysis</i>	12
Results	13
<i>Deforestation Trends</i>	13
<i>Forest Age Classification</i>	13
<i>Carbon Accumulation</i>	14
<i>Sub-Regional Analysis</i>	15
<i>Carbon Accumulation vs. other environmental variables</i>	15
Discussion	17
Conclusion	18
<i>Sources of Error and Suggestions for Further Study</i>	19
Acknowledgements	20
Works Cited	21

Figures and Tables.....	23
Appendix.....	50

Abstract

With heightened concerns about climate change and greenhouse gas emissions, understanding the mechanics of carbon sequestration is becoming more important than ever. The world's tropical forests are being sought for their increased ability to capture carbon in hopes that they might provide a solution to offset the emissions of industrialized nations.

Techniques for the promotion of carbon sequestration are being explored in all disciplines with plans spanning international markets. The Brazilian Amazon is of particular interest in these discussions, however comprehensive data on carbon sequestration in the region has yet to be seen, reducing the accuracy of estimates of potential carbon sequestered.

This study compared the carbon content of different-aged secondary forest stands to reach a deeper understanding of temporal trends in forest carbon sequestration using geospatial analysis and remote sensing techniques.

I used Landsat 5 Thematic Mapper satellite images to create a multi-temporal classification of forested and non-forested areas for 1984 to 2006. I then merged the classifications to estimate age the secondary forests present to the east of the Brazilian Amazon over this 22-year period. The resulting tree ages were compared to standing aboveground carbon based upon existing estimates from the Woods Hole Research Center's Pan-Tropical Forest Carbon dataset.

An increase in accumulated carbon for increasingly older secondary forests was observed over an area of 58,038 km². Deforestation rates in the study area have been generally decreasing since 1984, however in more recent years rising deforestation rates have been noted. Additionally, correlations were noted between carbon and latitude, precipitation, and temperature across the study area.

Introduction

Tropical forests are known to be important players in the process of climate change. The ability of forests in this region to sequester carbon has been a recent topic of exploration spanning fields of policy, international development, science, and economics, though comprehensive models are still largely unavailable. One of the barriers to programs such as the United Nation's Reduced Emissions from Deforestation and Forest Degradation program (REDD) is that the projected profitability from converting land to participate in carbon markets is often not comparable to the projected profitability of other land use (Butler et al., 2009). More accurate measures of the potential for a region to sequester carbon might allow researchers to better identify those regions that would in fact obtain long term benefits from participation in such programs.

Objective:

This study's preliminary focus was to determine secondary forest age across a study area of tropical forest in the eastern Brazilian Amazon. This data was then used to discern patterns in aboveground carbon accumulated over a period of time for four different age

classes. In this region, regrowth is occurring across a broad area while stands of primary forest still persist nearby. I used currently available carbon estimates, to determine accumulation of carbon from secondary forest regrowth across different-aged stands. The end product for this study is a model of aboveground carbon accumulation in secondary forests over time.

Deforestation and Climate Change:

Climate change, the increase in atmospheric greenhouse gas concentrations causing rising temperatures and changes in weather patterns, is one of the dominant environmental issues in politics and media today. Greenhouse gasses such as water vapor trap solar radiation inside the Earth's atmosphere, causing the planet to warm and influencing. The most noted of these gases is carbon dioxide (CO₂) (Malhi et al., 2002). CO₂ is composed of carbon, which is incidentally the primary component of organic matter and most living things. There are four main stores of carbon on our planet: geologic, oceanic, terrestrial, and atmospheric. Carbon moves through each of those stores in the carbon cycle. Carbon exists in rock carbonates, fossil organic matter (such as oil and coal), and geological reservoirs in the geologic stores, sediment and other components in the oceanic stores, plants and soil in the terrestrial stores, and compounds including carbon dioxide, methane, and other carbon-based gasses in the atmospheric stores (Malhi et al., 2002).

Forested ecosystems play an important role in the carbon cycle by annually cycling about 1/12 of total atmospheric carbon through the photosynthetic processes from production and respiration (Malhi 2002). Respiration (accounting for carbon loss of plants back into the atmosphere) typically cycles less carbon simultaneously than production (accounting for the

carbon harnessed by photosynthesis into biomass). The carbon use efficiency shows that, under ideal conditions, most plants uptake about 3-5 times the carbon they release at the same time (Larcher, 2003). This net gain allows plants to capture carbon out of the cycle for extended periods of time.

Anthropogenic deforestation reduces the number of available trees to uptake carbon while simultaneously increasing the rate at which carbon is released from plants through decomposition, burning, and the use of fossil fuels during extraction. This alteration causes the forest ecosystem to shift from a carbon sink to a source for atmospheric carbon. For example, if a tropical evergreen forest is converted to a pasture, the new ecosystem carbon pool can decrease to 40% the size of the original forest pool (representing combined above and below-ground carbon) (Kauffman, 2009). In the past decade, deforestation, occurring mainly in the tropics, has accounted for 12-20% of global anthropogenic carbon emissions annually (Paoli et al., 2010). Two to four percent of those global emissions are estimated to come from deforestation in the Brazilian Amazon (Helmer et al., 2009).

The role of forest management in Carbon Sequestration:

Carbon sequestration through reforestation can offset this effect, increasing the terrestrial carbon sink. Reserving areas to harness terrestrial carbon in the form of biomass will reduce the amount of carbon being cycled back into the atmosphere in the form of greenhouse gasses such as carbon dioxide or methane, thereby mitigating climate change.

The process of carbon sequestration utilizes forests to hold carbon in the stems of trees and woody plants. By planting more trees or protecting existing forested regions from being developed or transitioned to agricultural land, we can create or maintain carbon sinks. Old growth and new growth forests sequester carbon differently (Costa, 1996). For example, Figure 1 shows aboveground biomass (which is directly related to carbon content) over time since abandonment in an Amazonian stand from a study by Salimon and Brown (2000).

The biomass (and carbon) in young secondary forest increases with stand age until it begins to level off to an equilibrium. The age at which the rate of increase in carbon content becomes stable varies depending on a variety of factors including per plant photosynthetic rate, leaf area, solar radiation exposure time, water availability, plant structure, and density of sapling growth. The moist warm climate of the tropics is ideal for plant growth and so they have the highest net primary productivity (NPP) of any region on Earth (Larcher, 2003).

Achieving an adequate understanding of trends in the estimated carbon content of secondary Amazonian forest is important in determining the present value of Brazil's forest as carbon stocks for management practices to sequester carbon. Carbon sequestration projects such as voluntary carbon markets are a popular way for industries to offset their emissions. These industries invest indirectly in a forest management project to sequester carbon by purchasing carbon credits from an intermediary. These carbon credits represent carbon sequestered from these management projects. Accurate projections of carbon stocks for a plot of land could inform the land's value in future carbon credits or contribute to monitoring estimates in current projects. This sort of estimation and therefore the management that

follows can be significantly different depending on the types of trees (slow-growing high carbon versus fast growing low carbon) or other factors, and therefore the represented carbon should vary accordingly (Costa, 1996). Refining a methodology for determining the potential for carbon sequestration over a given time period on a plot-by-plot basis would be very useful for calculating the potential earnings from carbon markets.

Study Area

A study area was selected in Brazil due to the country's high historical clearing rates of tropical forests. This country is of interest because it is also committed to projects to reduce deforestation. For example, their National Plan on Climate Change boasts targeted elimination of net deforestation rates by 2015, as shown in Figure 2. This historic forest loss paired with the present initiatives toward reversal make Brazil a good candidate for this study as it focuses on the analysis of reforested areas. Additionally, despite the potential for forests in this region to sequester carbon, there has not been a lot of quantitative research performed on this topic at this location, and so accurate models have not been developed showing trends for the area (Hayes et al., 2009).

The 300m GlobCover dataset, derived from data from ENVISAT's Medium Resolution Imaging Spectrometer (MERIS) was used to assess land cover change in the region (Bontemps, 2010). The study area was refined to a region with a large amount of recent conversion from croplands or cleared lands to forest shown in Figure 3.

The selected study area, mapped in Figure 4 is a region of mixed tropical forest on the border of the Amazon. The region I chose covers 58,038 km² and is located to the east of Para just north of Tocantins. The main land cover types in the area are for crop fields and deciduous forest (Figure 5). The mean annual precipitation within my study area is 1,907 mm/y (Figure 6) and the mean annual temperature is about 29.3 degrees Celsius (Figure 7). Elevation within the study area ranges from 34-771 meters (Figure 8). There is a mild dry season in the region between August and October (Feldpausch et al., 2004).. Because of its large size, the study area was also broken into sub-regions to look at relationships on a smaller spatial scale. Ten sub-regions were drawn, numbered 0-9 (Figure 9).

Methods

Forest ages were determined by classifying satellite images by land cover type of interest (in this case, forest and non-forest) and then resulting classifications were synthesized to determine when forests initially developed for each pixel over time. This data was compared to the Woods Hole Research Center's pan-tropical carbon dataset to assess of carbon content across each age class. Patterns of carbon and age were further analyzed against a number of environmental variables to determine trends. All image processing was performed using ArcGIS, ENVI, and the arcpy module in python.

Data selection:

I obtained LANDSAT 5 images from the National Institute for Space Research (INPE) and USGS's Earth Explorer. The study area was the size of two 170 km x 185 km Landsat footprints

in path 223 and rows 63-64 with a 30x30 pixel resolution (in all bands utilized in this study). Images were selected with less than 10% cloud cover.

I chose five images between the earliest available date (1984) and 2006, corresponding to the date associated with the carbon dataset used for comparison at intervals close to every five years. Additionally, images were selected in 2010 (path 223, row 64) and 2011 (path 223, row 63) for deforestation analysis. I selected images to fall before the dry season in October in order to reduce the influence of soil moisture in the images and to reduce interference from clouds, while still maintaining an optimal leaf area for satellite detection. Additionally I made an effort to select for anniversary dates where possible to reduce the influence of seasonal phenological changes and sun angle (Singh, 1989, Coppin and Bauer, 1994). Most image dates fell in early June, but a significant number fell in late July (Figure 10).

A pan-tropical forest carbon dataset, produced by the Woods Hole Research Center was used to summarize the total carbon within each age class and discern trends. This 500m dataset draws from a model relating waveform LiDAR (IceSAT/GLAS) with field measurements, and MODIS imagery (used to scale up and extend the GLAS biomass estimates to a wall-to-wall map dataset) with validation from SPOT imagery. It was created to inform REDD negotiations (WHRC, 2010, 2011). This dataset was selected because it is a publically accessible dataset using state of the art technology and provides current carbon estimates. Because it is expressed in biomass, this dataset was scaled by 0.4809 before compared to forest age. (Jaramillo et al., 2003)

Data for precipitation and temperature were obtained from the WorldClim dataset (citation- Hijmans, elevation data was obtained from the United States Geological Survey's

(USGS) Global Multi-Resolution Terrain Elevation Dataset (GMTED), land cover was obtained from the European Space Agency's (ESA) GlobCover dataset, and protected areas were obtained from the World Database of Protected Areas (Table 1).

Pre-processing:

I radiometrically and atmospherically corrected the images using landsat calibration and dark object subtraction with I_{min} and I_{max} values from the calibration values provided in Chander, 2009. I georectified all images to the 1990 dataset selecting this year because this date fell toward the middle temporal range in hopes that many of the same features would be available allowing for repeated use of ground control points (GCPs) for each image. Between 20 and 25 GCPs were selected to achieve a root mean squared (RMS) error below 2 (Table 2). In addition to achieving RMS errors less than 2.0, image registration was verified visually.

Forest Ageing through Post-Classification Merging:

I chose to use a post-classification merging approach for detecting differences in forest cover because I did not have the ground truth resources available to determine spectral thresholds for image differencing (Hayes and Sader, 2001). Additionally, this method is known to reduce the influence of atmospheric differences between dates (Lu et al., 2002). This approach requires an image classification (supervised or unsupervised) for each time series image in the study. These images are then synthesized using a comparative approach. For this study images were merged, tracking forest ages based on

presence-absence data from classified images across the time period (Helmer, et al. 2009) (Figure 11).

My image classification included three classes: Forest, non-forest, and clouds and no data. Values classified as “No Data” correspond to pixels affected by cloud cover or where separation between forest and non-forest was not clearly discernible, so rather than lumping those pixels into a class that they did not belong, they were left unclassified. For example, some regions of very bright agriculture or bare soil might have a small number of pixels considered to have “No Data” attributed to them. Both cloud cover and “No Data” pixels from each image in the time series were completely removed from the final age raster, and replaced with “No Data” values because pixels in those classes needed to be excluded from the final age classification due to the inability to determine whether regions beneath clouds were in fact forested or not

For each Landsat image, I derived the normalized difference vegetation index (NDVI) and classified the images based on the combination of this data as well as values in bands 2, 3, 4, and 5.

I experimented with classification methods Using Landsat images from 2010, two methods were tested to classify the images, including maximum likelihood supervised classifications and Isodata unsupervised classifications. Bands 2, 3, 4, 5, and the NDVI transformation were input into both classifications. Some experimentation using the second Principal Component band (PCA band) was done, but it was determined that the high covariance between this data and the NDVI limited the accuracy of the classifications.

Additionally, Lee’s method was tested to identify a threshold the NDVI layer (Lee, 2008), however this method was very time consuming and frequently mis-classified fallow

crop fields as forested areas. This method proved to be too unwieldy given the scale of this project and the diversity of the images.

The maximum likelihood supervised classification was run with a probability threshold of 0.4 and an input of 22 classes. After classification these 22 classes were then combined to three classes (clouds and no data, non-forest, and forest).

Accuracy of both the supervised and unsupervised methods (with and without post-processing) was assessed by comparing each classification method from 2010 to Google Earth imagery at 100 randomly generated points scattered throughout the study area. The chosen metric to determine accuracy was Cohen's kappa value (κ) (Fielding and Bell, 1997). Kappa was calculated from this comparative data for each classification method (Table 3)

While the outputs were similar from these two classifications, based on kappa values, the more accurate method for classifying the land cover types in this study was the IsoData unsupervised classification, run for three iterations with a minimum of ten pixels per class. This classification called for 50-100 classes which were later sorted and merged accordingly into the three classes. The unsupervised classification yielded a higher kappa value than the supervised classification.

Once each of the images was reclassified into three classes, I assessed the difference between each pair of sequential images to determine deforestation and reforestation areas and rates. I also synthesized the classified images to track the forest ages across the years (Lee, 2008). This dataset was also reclassified to show deforestation in the study area at each time step and separately between only the first and last dates to show net change.

Analysis:

Data values and summary statistics for the carbon content of each forest age class were drawn from the pan-tropical carbon dataset by age class for 10,000 random points distributed across the study area. Out of these 10,000 points 1994 landed in regions of secondary forest that were not classified as “No Data” or clouds and were therefore usable. These data were then graphed in a box plot comparing forest age to carbon content at each point.

Carbon values for all pixels in the study area were then plotted in histograms by age range to observe the relative distributions of the data. Pixels with a carbon value of 0 MgC/ha excluded from these histograms to improve visibility of trends across the full range of carbon values, but remain in all other analysis.

Carbon content was also plotted against a number of other variables including mean annual temperature, mean annual precipitation, elevation, latitude, and longitude to determine possible underlying influences. Latitude and longitude were defined based on the World Robinson projected coordinate system.

Carbon accumulation at different forest ages was analyzed by sub-region. 10,000 random points were generated in each sub-region and boxplots were generated comparing carbon to forest age for each group. Breaking the study area down into smaller sub regions should account for some of the possible interference from trends in precipitation, elevation, and other spatially related environmental factors which may influence carbon sequestration (Chazdon et al., 2007) as well as influences from land use and intensity prior to reforestation as studies have shown significant differences in the ability of forests to

uptake nutrients from shifting cultivation and cattle pasture (Fearnside and Guimarães, 1996).

Results

Deforestation Trends:

Initial analysis shows that deforestation rates were highest from 1984 to 1990 (Figures 12 and 13). Between the years of 2001 and 2006 the analysis shows the highest rate of regrowth and the lowest rate of deforestation of the time periods studied. The general trend shows decreasing deforestation, however there has been a slight reversal in this trend between 2006 and 2010.

Forest Age Classification:

A mosaic of different aged forest stands was found interspersed throughout the study area with a few regions with dominant age classes for the year 2006 (Figures 14 and 15). In the northern portion of the study area there is a sizeable forested region comprised mostly of secondary forest under five years old (purple) surrounding a region dominated by primary forest (green) to the south. The regions showing “No Data” were either left unclassified or were omitted due to interference by clouds or water bodies during any of the years analyzed (24% of the study area). Primary forest and non-forest areas constitute 11% and 48% of the area respectively, while 17% of the study area is classified as secondary forest (Figures 16).

Land cover percentages for individual classifications show similar trends (Figure 17). In 2006, the majority of the secondary forest in the study area was between 1 and 5 years old, while forests between 10-and 21 years comprise a much smaller area (Figure 18).

Carbon Accumulation:

An overall trend of increasing carbon content with forest age was found (Figure 19). Stands aged 0-5 years occupy 54.9% of the secondary forest area as of 2006. Forests between ages 0 and 5 were found to have a greater interquartile range (shown by the extent of the box in the box plot) than other age classes, indicating a higher variability of carbon values within the class. Pearson's correlation coefficients show no correlation (Table 4).

The distribution of the carbon values across all secondary forests is multimodal, with various peaks (Figure 20). Noting the relative areas of age classes within the study area which causes those distributions to appear higher overall in the histogram, young stands aged 0 to 5 have more high-carbon content pixels than older stands (Figure 21). Excluding values of 0 MgC/ha, the most prevalent carbon value for stands aged 0 to 5 is 350 Mg/ha (figure boxplot?), the mode for stands aged 5-11 is at 162 Mg/ha with another peak around 100 Mg/ha, the mode for stands aged 11-16 falls at 162 Mg/ha and the mode for stands aged 16-22 falls at 352 Mg/ha. Additionally there is a gap from 250-290 MgC/ha where little data exist. This gap is present across the whole study area regardless of stand age, and perhaps is an artifact of the original carbon layer.

Sub-regional Analysis:

On a sub-region scale, carbon accumulation was observed to increase with forest age for many of the regions (Figure 23). Exceptions include sub-regions 1 and 2, which have lower than expected values for ages 16-22, and sub-regions 8 and 9 which have higher than expected values for ages 0-5. Sub-region number roughly follows latitude with higher sub-region numbers having higher carbon overall (Table 6).

Sub-regional comparisons between carbon and forest age showed overall higher correlations than comparisons for the entire study area based on Pearson's product-moment correlation coefficient (Tables 4 and 6). Sub-region 8 was the only sub-region which did not have a higher correlation coefficient than the study area as a whole, and sub-regions 4, 6, and 7 actually showed significant correlations between forest age and carbon (Table 6).

Additionally, the two dominant land cover types appear to distinguish sub-regions 0-4 from sub-regions 5-9, and primary forest dominates sub-regions 2,3,5,6, and 7, while the remaining sub-regions are dominated by forests aged 0-5 (Table 6).

Carbon Accumulation vs. other environmental variables:

When carbon was compared with other environmental variables carbon content was observed to be significantly correlated to increases in higher latitude, longitude, and precipitation, while it appeared to be less by temperature and elevation (Table 5; Figure 22).

While carbon varies widely across all precipitation values, there is a generally increasing trend (Table 5; Figure 22). Higher volume areas of the plot appear to move in an upward direction with carbon and precipitation increasing directly. A cluster exists in the data at around 150 Mg C/ha corresponding to precipitation values greater than 1850 mm/y. This exists in all plots, and is not particular to the comparison of carbon to precipitation.

Comparing carbon accumulation to temperature shows that the majority of the points taken from the study area have a mean annual temperature that is greater than 25.5 degrees Celsius. Carbon values show a limited visible correlation, despite the significant correlation coefficient. Here, the cluster at 150 MgC/ha corresponds to temperature values between 26.2 and 27 degrees Celsius.

Elevation shows an even more concentrated arrangement of points than temperature, however most of the data appears to be concentrated at low elevations. The full range of carbon values can be seen across a very small range in elevations, producing a plot with little or no correlation. The correlation coefficient is less than 0.2, and reflects the lack of relationship between carbon and elevation.

The highest correlation exists between carbon content and latitude. Carbon visibly increases at higher latitudes. This relationship showed the highest correlation coefficient of all variables tested. The cluster at 150 Mg C/ha corresponds to latitudes in the upper 20% of the study area.

There is little correlation between longitude and carbon with a wider arrangement of carbon values across all longitudes. The cluster (Figure 22) appears to encompass more of the

higher carbon values, but stretches across a wide range of latitudes. The correlation coefficient for carbon vs. longitude shows no correlation.

Discussion:

While deforestation rates have shown considerable decreases since 1984, forest loss is still an issue in Brazil and significant effort will be required to reduce the effects. In recent years the data show an increase in deforestation. This could possibly indicate the presence of forested areas that are not maintained regularly, but are cut every few years for some purpose. This could also explain the result that forests aged 0-5 cover more of the study area than other secondary forest ages. This large area of young secondary forests may also be a result of increased reforestation efforts.

The presence of a portion of the primary forest found in the study area can be explained by the existence of protected areas. The majority of all protected area within the study area is primary forest. These forests dominate many of the larger protected areas. Many of the smaller protected areas are dominated by younger secondary forests, and have been established more recently. The recent establishment of many protected may be further evidence of Brazil's efforts toward protecting their forests (Table 7).

In general, I found that average carbon content increases with increasing forest ages, with the exception of the youngest forest class (0-5 years). All age classes had a very wide range of values especially the youngest forests. The variability in all classes is likely due to the scale of the study area and the incredible variation in land use and environmental conditions which can exist across such a large area. It is likely that the wide range of carbon values within

the same age class reflect the variable carbon sequestration trends based on different historic land use, such as those shown between shifted cultivation and pasture land cited by Fearnside and Guimarães (1996).

The correlation between carbon and precipitation values reflects known trends in net primary productivity across precipitation gradients. Huxman et al. (2004) compiled data comparing aboveground net primary productivity (ANPP) to annual precipitation across a number of biomes (Figure 24: indicated by abbreviations). The tropical forest biome represented in this study is most closely related to Barro Colorado Island (BCI) which actually has a negative relationship between ANPP and precipitation, yet geographic scale and range of precipitation values are not directly comparable.

While sub-regions with similar values for carbon did not seem to show similar elevation, precipitation, or temperature values, they did appear to have a limited relationship to land cover type and dominant forest age. Carbon values generally increased as sub-regions progressed further north in latitude. The association between carbon and latitude was shown in both sub-regional analyses, as well as in the correlation of carbon to latitude, where the correlation coefficient showed a moderate relationship.

Conclusions:

Determining temporal trends in forest dynamics and resulting standing carbon over such a large study area is a daunting task with large amounts of uncertainty. Regardless, predictable trends were observed of increasing carbon content with secondary forest age for the entire

study area. When the study area was categorized spatially by sub-region, the different relationships between carbon and forest age across geographic areas became apparent.

Further, carbon content showed some correlation with precipitation and temperature, and moderate correlation with latitude, indicating that carbon accumulation may vary under different climactic conditions or with even small variation in distance from the equator. This analysis also showed that primary forests are the main target for protection in this part of Brazil. Forest regrowth rates have been increasing, and many of the established protected areas appear to perpetuate this trend as well.

Sources of Error and Suggestions for Further Study:

Post-classification comparison techniques, such as the one I have used in this study, have the disadvantage of compounding errors throughout each step of analysis. Errors in the initial classification can lead to errors in the change detection (Kennedy et al., 2009).

Further, to more accurately express forest age it may be wise to research the minimum age of detection by satellite for forests. Lee, 2008 cites an “NDVI-age” of 15 years for evergreen trees as the minimum age at which a Landsat-based NDVI transformation to detect such a tree. It is likely that the trees detected in the IsoData classification were significantly older than indicated in the analysis, and so if trends derived from satellite data were to be used in management they would not reflect a real scenario. Setting a baseline age would give a more accurate estimation.

Data on historic land use is incredibly important when understanding carbon accumulation in forests, especially at larger spatial scales. Research into historic land use in tropical systems would be recommended for comparison of these trends.

Acknowledgements:

I would like to express my sincere gratitude to all those who assisted me with this project. Firstly, I would like to thank my advisor, Dr. Jennifer Swenson for her patience, guidance, and advice throughout this project. I would like to thank the Woods Hole Research Center for providing me with access to their data, without which this project would not be possible. In particular, I would like to thank Greg Fiske and Dr. Alessandro Baccini.

I would also like to extend my gratitude to the professors and staff at the Nicholas School of the Environment for their efforts to make this program what it is, and my peers at the Nicholas School for their support.

Works Cited

- Bontemps, S., et al. *GlobCover 2009 Product Description Manual*. European Space Agency. (2010) Accessed from: http://ionia1.esrin.esa.int/docs/GLOBCOVER2009_PDM_1.0.pdf
- Butler, R, L. P. Koh, and J. Ghazoul. *REDD in the red: palm oil could undermine carbon payment schemes*. Conservation Letters 2. Wiley Periodicals.
- Byrne, G.F., P.F. Crapper, and K.K. Mayo (1980). *Monitoring Land-Cover Change by Principal Component Analysis of Multitemporal Landsat Data*, Remote Sensing of Environment, VOL. 10, 175-184.
- Chander, G., B.L. Markham, and D.L. Helder (2009). *Summary of current radiometric calibration coefficients for Landsat MSS, TM, ETM+, and EO-1 ALI sensors*. Remote Sensing of Environment, Vol. 113, pp. 893-903.
- Chazdon, R., et al. *Rates of change in tree communities of secondary Neotropical forests following major disturbances*. Philosophical Transactions of the Royal Society, Vol. 362 No. 1468 (February 28, 2007), pp. 273-289
- Coppin, P. R., and M. E. Bauer (1994). *Processing of Multitemporal Landsat TM Imagery to Optimize Extraction of Forest Cover Change Features*, Transactions on Geoscience and Remote Sensing, IEEE, Vol. 32, no.4, pp. 918-927.
- Costa, P.M. (1996) *Tropical Forestry Practices for Carbon Sequestration: A Review and Case Study from Southeast Asia*. Royal Swedish Academy of Sciences. Ambio, Vol. 25. No. 4. Pp. 279-283.
- Dewar, R.C. (1990) *A model of carbon storage in forests and forest products*. Tree Physiology. Vol. 6. Pp. 417-428.
- Fearnside, P.M. and W.M. Guimarães. (1996) *Carbon uptake by secondary forests in Brazilian Amazonia*. Forest Ecology and Management. Vol. 80. 35-46.
- Feldpausch, T.R., M.A. Rondon, E.C.M. Fernandes, S.J. Riha, and E. Wandelli. (2004) *Carbon and Nutrient Accumulation in Secondary Forests Regenerating on Pastures in Central Amazonia*. Ecological Applications. Vol. 14. No. 4. Supplement 2004. S164-S176.
- Fielding, A.H. and J.F. Bell. (1997) *A review of methods for the assessment of prediction errors in conservation presence/absence models*. Environmental Conservation. Vol 24. No. 1. Pp. 38-49.
- Goetz, S., & Fiske, G., *Linking the diversity and abundance of stream biota to landscapes in the mid-Atlantic USA*, Remote Sensing of Environment (2008), doi:10.1016/j.rse.2008.01.023
- Hayes, D.J., and S.A. Sader (2001) *Comparison of Change Detection Techniques for Monitoring Tropical Forest Clearing and Vegetation Regrowth in a Time Series*, Photogrammetric Engineering & Remote Sensing, VOL. 67. No. 9, 1067-1075.
- Huxman, T.E., et al. (2004) *Convergence across biomes to a common rain-use efficiency*. Letters to Nature. Nature. Vol. 429.

- Instituto Nacional de Pesquisas Espaciais (INPE). (2009) *PRODES: Assessment of Deforestation in Brazilian Amazonia*. Natl. Inst. For Space Res. São José dos Campos, Brazil. www.inpe.br
- Jaramillo, V.J., et al. (2003) *Biomass, Carbon, and Nitrogen Pools in Mexican Tropical Dry Forest Landscapes*. *Ecosystems*. V 6. Pp 609-629.
- Kauffman, J.B. et al. *Carbon pool and biomass dynamics associated with deforestation, land use, and agricultural abandonment in the neotropics*. *Ecological Applications*, Vol. 19, No. 5 (2009), pp. 1211-1222
- Kennedy, R.E. et al., *Remote sensing change detection tools for natural resource managers: Understanding concepts and tradeoffs in the design of landscape monitoring projects*, *Remote Sensing of Environment*, VOL.113, 1382-1396.
- Larcher, W. *Physiological Plant Ecology*. 4th Edition. (2003) Springer. Berlin. Pp. 140.
- Lee, H. (2008). *Mapping Deforestation and Age of Evergreen Trees by Applying a Binary Coding Method to Time-Series Landsat November Images*. *Transactions on Geoscience and Remote Sensing, IEEE*, VOL. 46, no.11, 3926- 3936.
- Lu, D. et al. (2003) *Change Detection Techniques*, *International Journal of Remote Sensing*, VOL. 25, no. 12, 2365-2407.
- Malhi, Y., et al. *Forests, Carbon and Global Climate*. *Philosophical Transactions of the Royal Society: Mathematical, Physical, and Engineering Sciences*, Vol. 360, N. 1797, carbon, Biodiversity, Conservation and Income: An Analysis of a Free-Market Approach to Land-Use Change and Forestry in Developing and Developed Countries (Aug. 15, 2002), pp. 1567-1591
- Paoli, G. et al. *Biodiversity Conservation in the REDD*. *Carbon Balance and Management*, Vol. 5 No. 7. (2010)
- Salimon, C., & Brown, F., *Secondary Forests in Western Amazonia: Significant Sinks for Carbon Released from Deforestation?*. *Interciencia*, Vol. 25, N. 4. (July 2000), pp. 198-202
- Singh, A. (1989). *Review Article: Digital change detection techniques using remotely-sensed data*, *International Journal of Remote Sensing*, VOL. 10, no 6, 989-1003.
- Smith, J.E.; Heath, Linda S.; Skog, Kenneth E.; Birdsey, Richard A. 2006. *Methods for calculating forest ecosystem and harvested carbon with standard estimates for forest types of the United States*. Gen. Tech. Rep. NE-343. Newtown Square, PA: U.S. Department of Agriculture, Forest Service, Northeastern Research Station. 216 p.
- Terborgh, J. *The Vertical Component of Plant Species Diversity in Temperate and Tropical Forests*. *The American Naturalist*, Vol 126, No. 6. (Dec. 1985) pp760-776.
- WHRC. *Pan-Tropical Forest Carbon Mapped with Satellite and Field Observations*. Mapping and Monitoring. Woods Hole Research Center. WHRC.org. (2011) Accessed from: <http://www.whrc.org/mapping/pantropical/modis.html>
- WHRC. *Pan-Tropical Mapping of Forest Cover and Above-Ground Carbon Stocks (2009-2011)*. SPOT Planet Action Report. (August 2010)

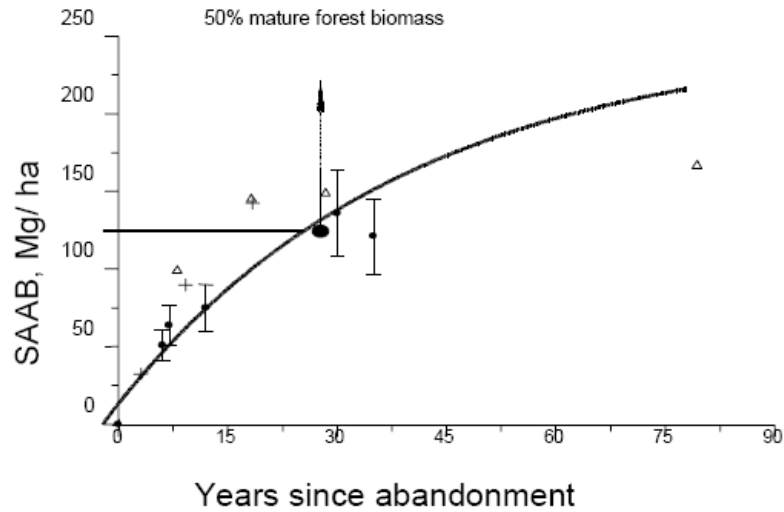


Figure 1: From Salimon and Brown (2000). “Standing Alive Aboveground Biomass (SAAB) in secondary forests as a function of years since abandonment. Error bars show estimated 20 percent uncertainty in SAAB measurements. Curved line is best fit for the equation $SAAB = 250 * (1 - \exp(-0.025 t))$ in $Mg * ha^{-1}$. The independent variable, t , is in years. Dotted line at $125 Mg * ha^{-1}$ indicates that half the mature forest biomass is reached in less than 30 years. The study sites are near Rio Brance, Acre, Brazil. Full circles with error bars: data from present study; triangles: data extracted from Fearnside and Guimarães (1996); crosses: data from Alves et al. (1997).”

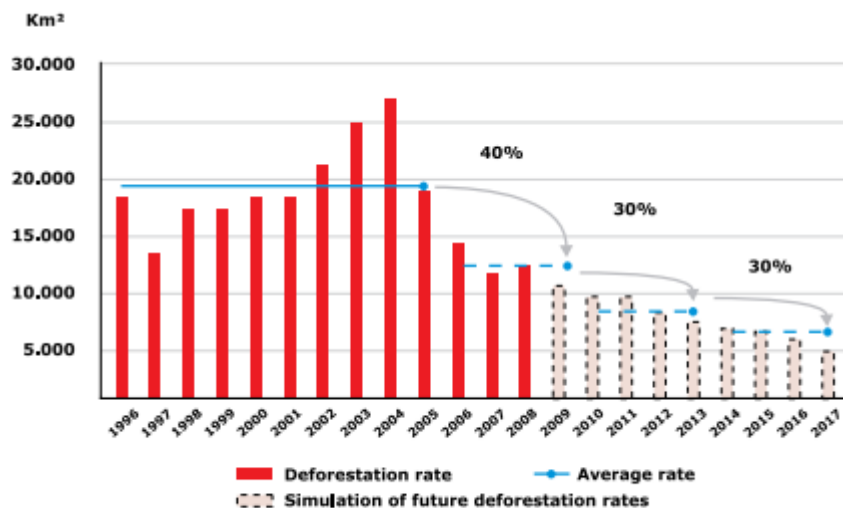


Figure 2: Past trends and projected goals for deforestation in Brazil. (INPE, 2009)

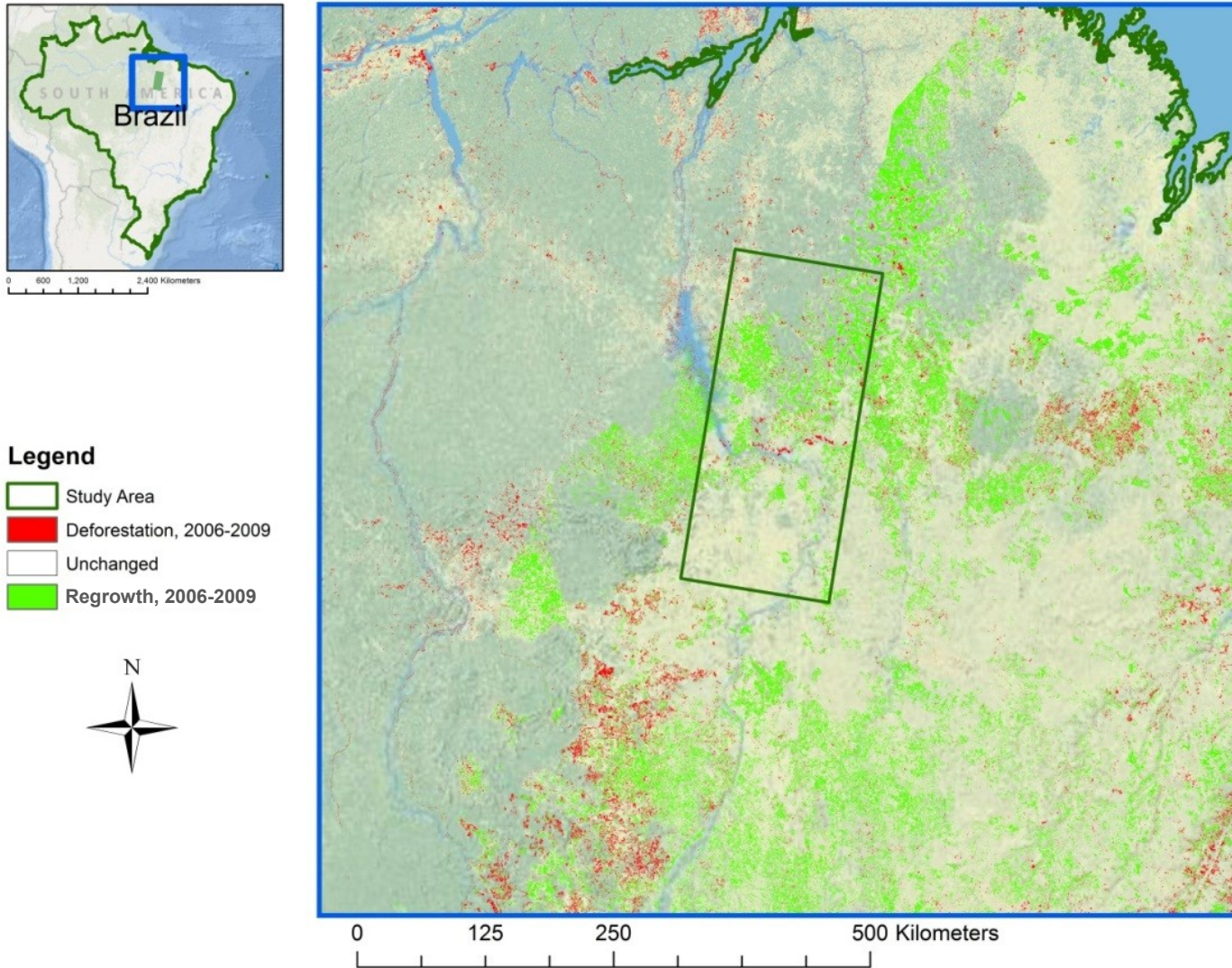


Figure 3: Study area selection encompassing regions of forest regrowth derived from changes in the GlobCover 2006 and 2009 datasets. Background: ESRI Ocean Basemap.



Figure 4: Study area located on the Eastern border of the Amazon tropical forest. Background: ESRI Ocean Basemap.

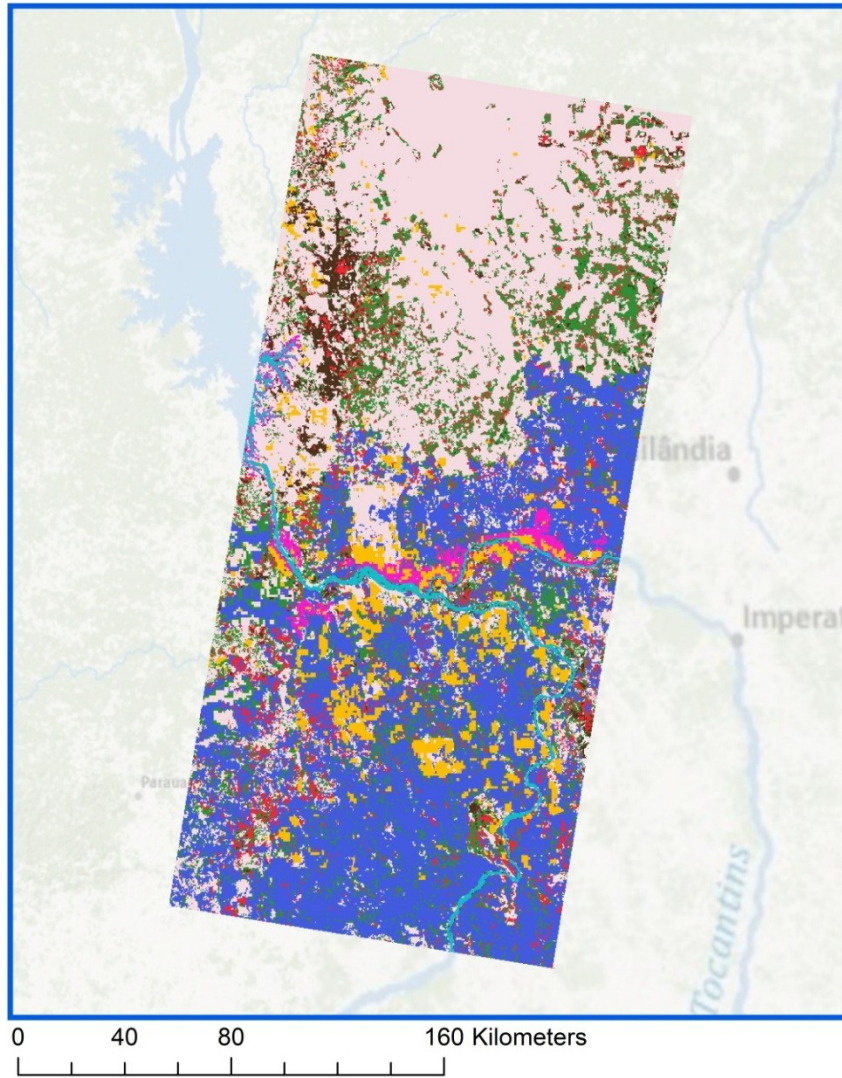


Figure 5: Land Cover in study area (GlobCover), 2006. Background: ESRI Ocean Basemap.

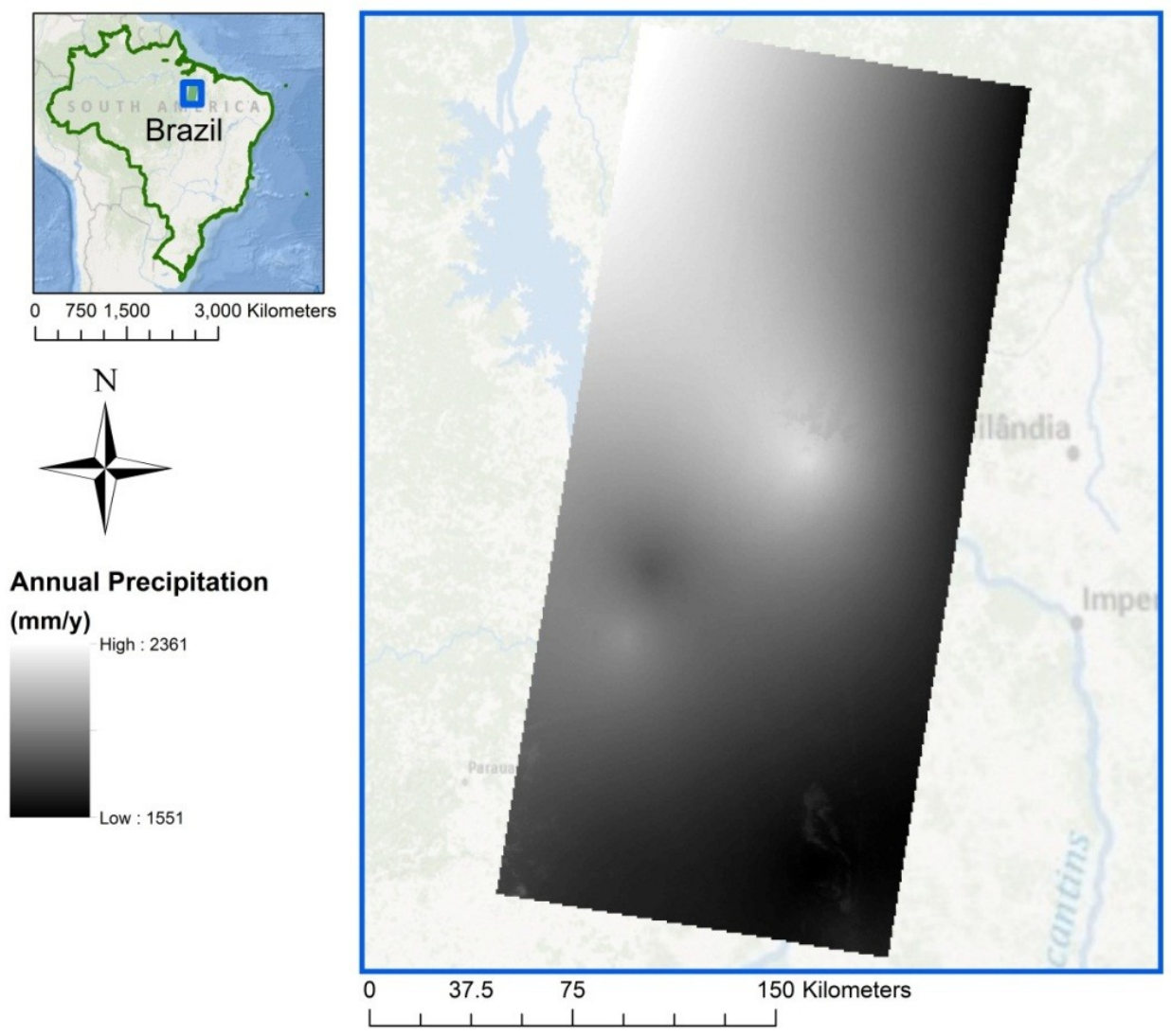


Figure 6: Annual Precipitation in study area (WorldClim). Background: ESRI Ocean Basemap.

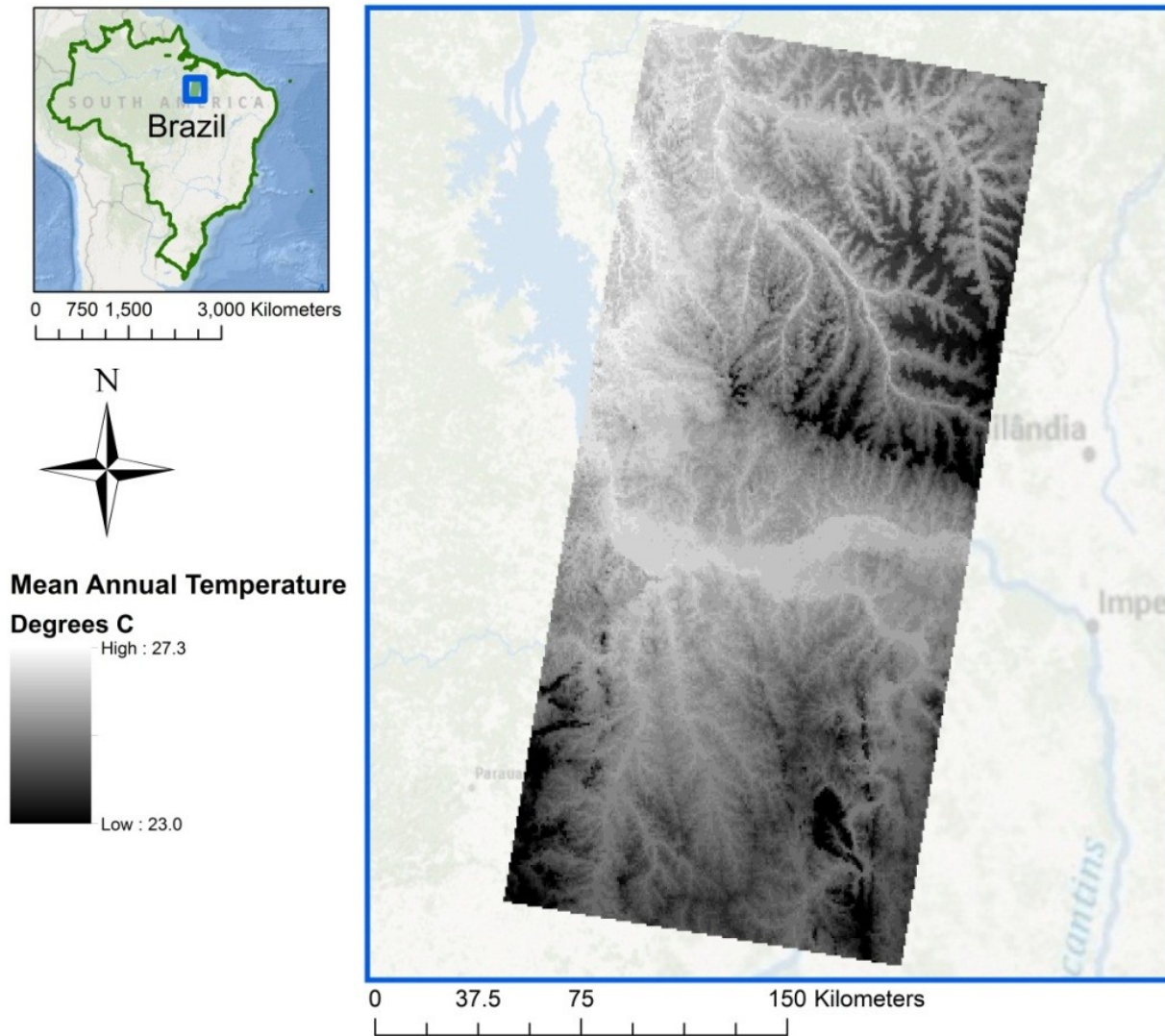


Figure 7: Mean annual temperature in study area (WorldClim). Background: ESRI Ocean Basemap.

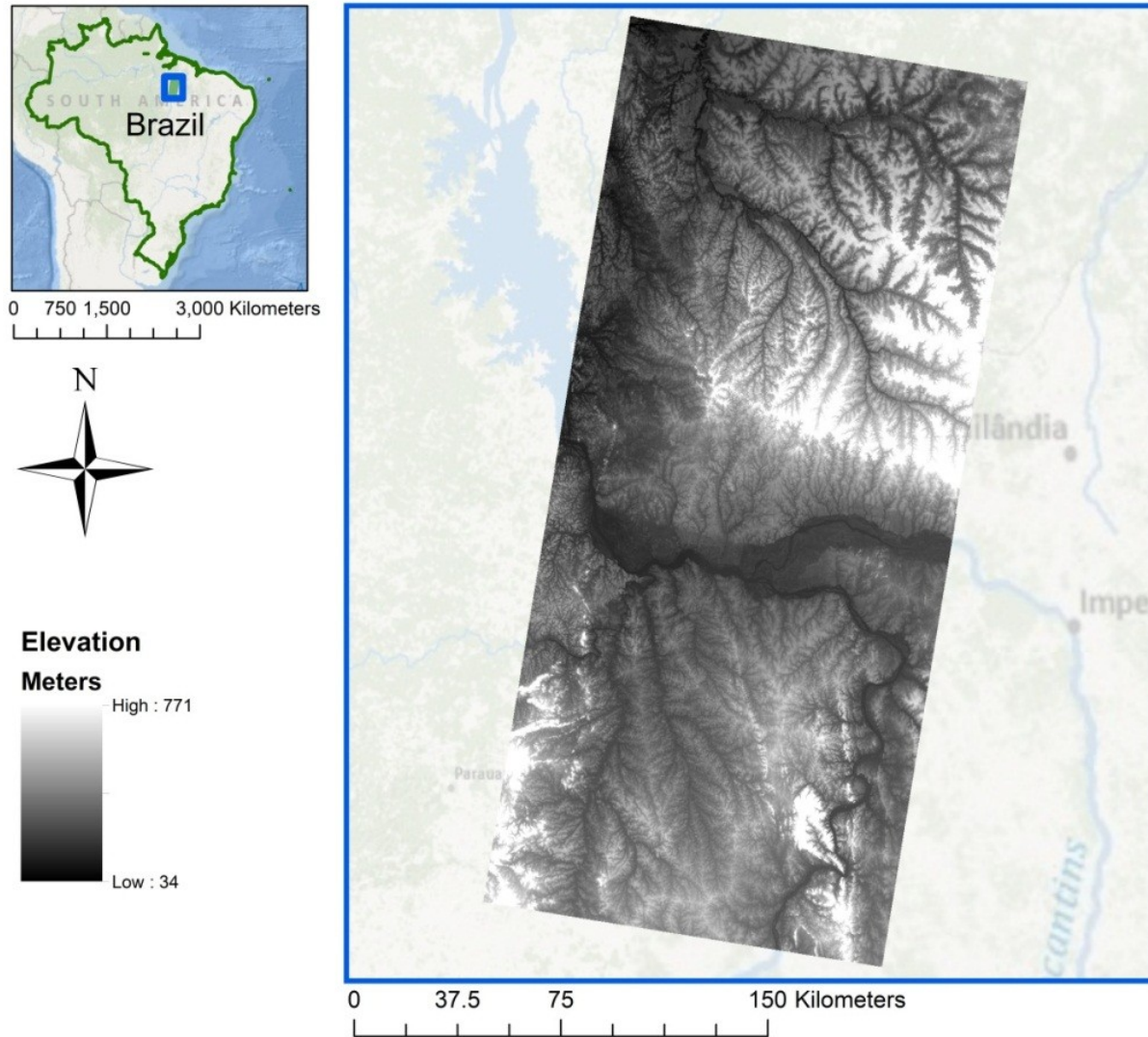


Figure 8: Elevation in study area (GMTED). Background: ESRI Ocean Basemap.

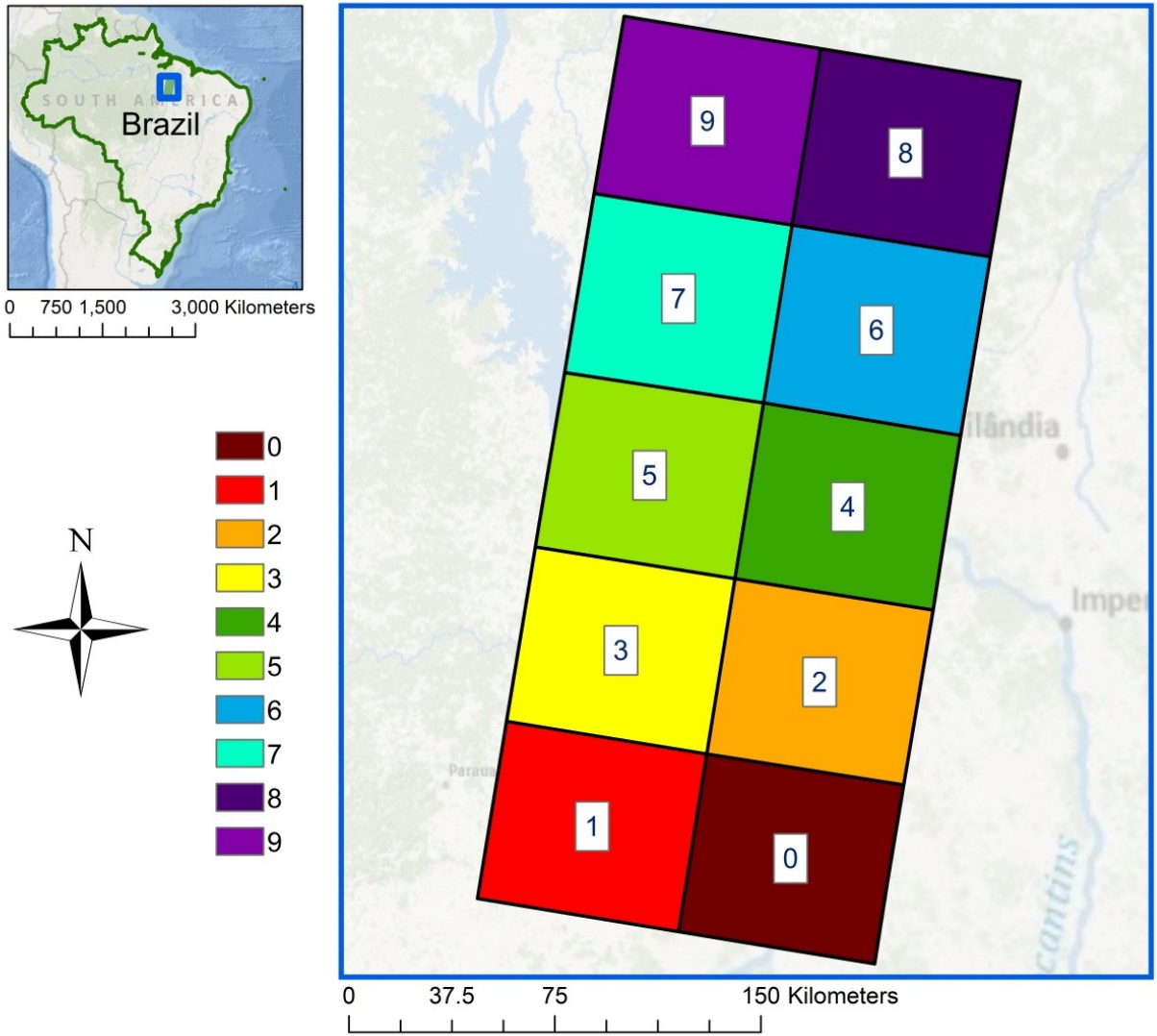


Figure 9: Sub-regions of study area. Background: ESRI Ocean Basemap.

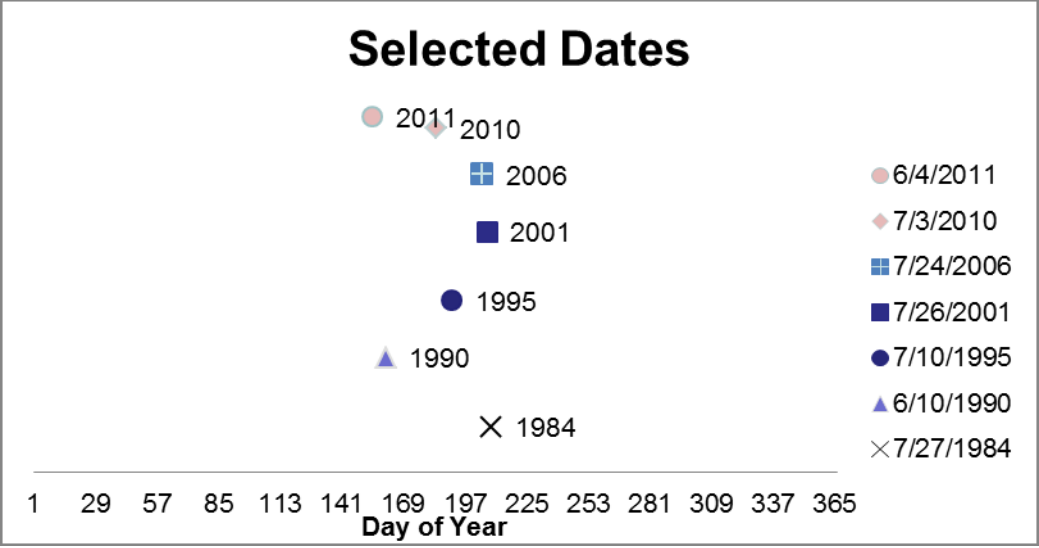


Figure 10: Selected dates of Landsat images for use in determining forest ages are shown in blue. Additional dates in pink were used to determine deforestation and reforestation areas. (2010 date was in path 223 and row 64 and 2011 date was in path 223 and row 63). X axis represents day of year so difference in points' horizontal location shows difference in calendar date.

Layer Type	Name	Resolution	Access Source
Elevation	Global multi-resolution terrain elevation dataset (GMTED)	30 arc seconds	USGS Earth Explorer
Precipitaion	WorldClim, Annual Precipitaion	30 arc seconds	WorldClim.org
Temperature	WorldClim, Annual Mean Temperature	30 arc seconds	WorldClim.org
Carbon	Woods Hole Research Center's Pan-Tropical Carbon Dataset	500 m	Not publically accessible, information at WHRC.org
Protected Areas	IUCN and UNEP-WCMC World Database of Protected Areas	Unknown	ProtectedPlanet.net
Basemap	ESRI Oceans Basemap	Multiple, Unknown	ArcMap Basemaps
Satellite Imagery	Landsat 5 TM	30 m	USGS Earth Explorer and INPE

Path, Row	Date	RMS Error
223, 63	7/27/1984	0
223, 63	6/10/1990	N/A
223, 63	7/10/1995	0.882018
223, 63	7/26/2001	1.39993
223, 63	7/24/2006	1.579219
223, 63	6/4/2011	1.529075
223, 64	7/27/1984	0
223, 64	6/10/1990	N/A
223, 64	7/10/1995	1.342612
223, 64	7/26/2001	1.410592
223, 64	7/24/2006	1.409915

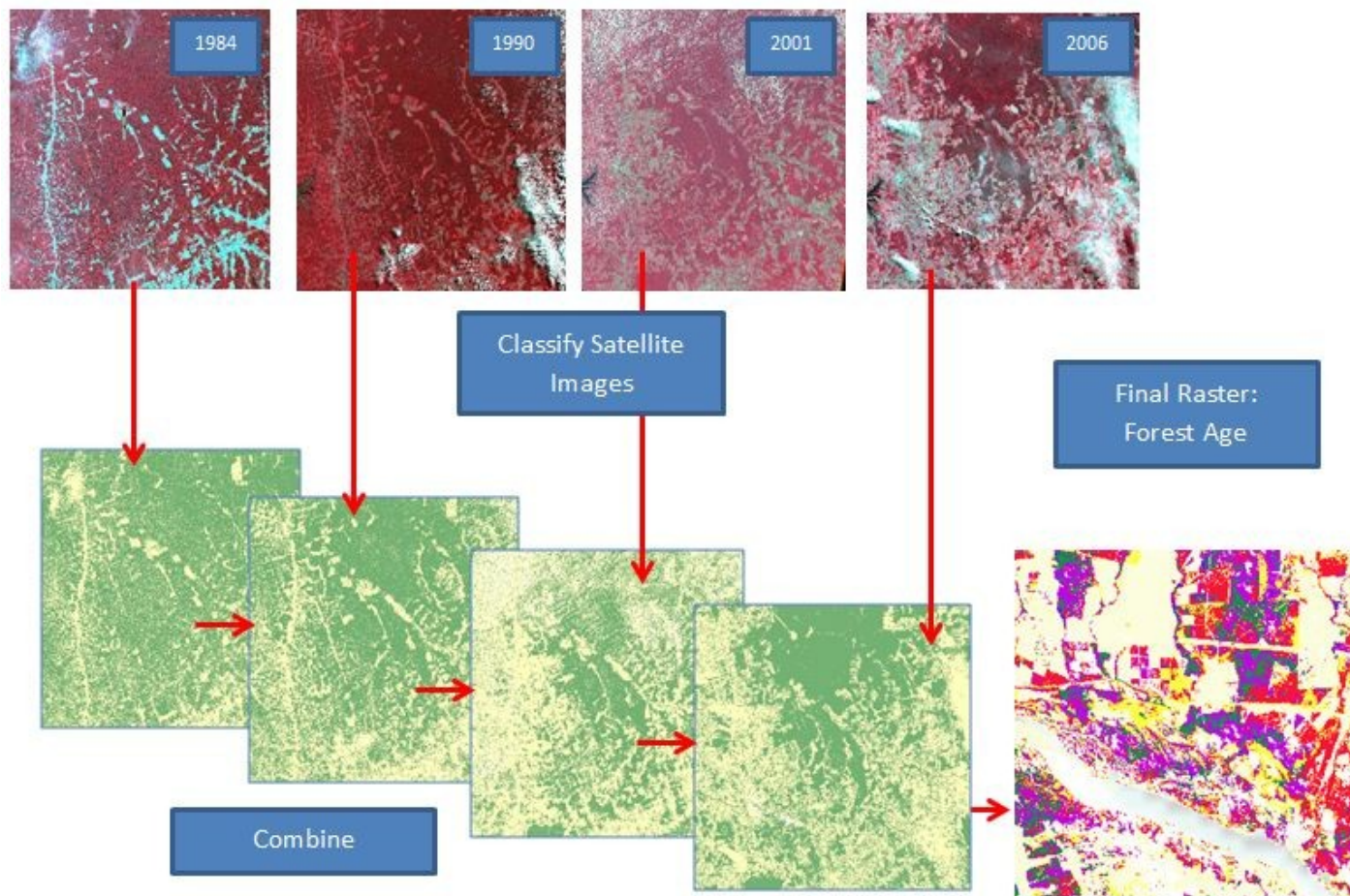


Figure 11: A schematic of the post classification merging method used to determine forest age.

Table 3: Confusion matrices from each classification method with kappa and percent accuracy.

		Actual			
		Forest	Non-Forest	Kappa	% Accuracy
Predicted	Unsupervised				
	Forest	32	9	0.627945	82
	Non-Forest	9	50		
	No Data	0			
	Unsupervised with Post-Processing				
	Forest	32	9	0.584435	81.25
	Non-Forest	9	46		
	No Data	4			
	Supervised				
	Forest	29	11	0.613003	83.33
	Non-Forest	5	51		
	No Data	4			
	Supervised with Post-Processing				
	Forest	28	12	0.618321	84.21
	Non-Forest	3	52		
	No Data	5			

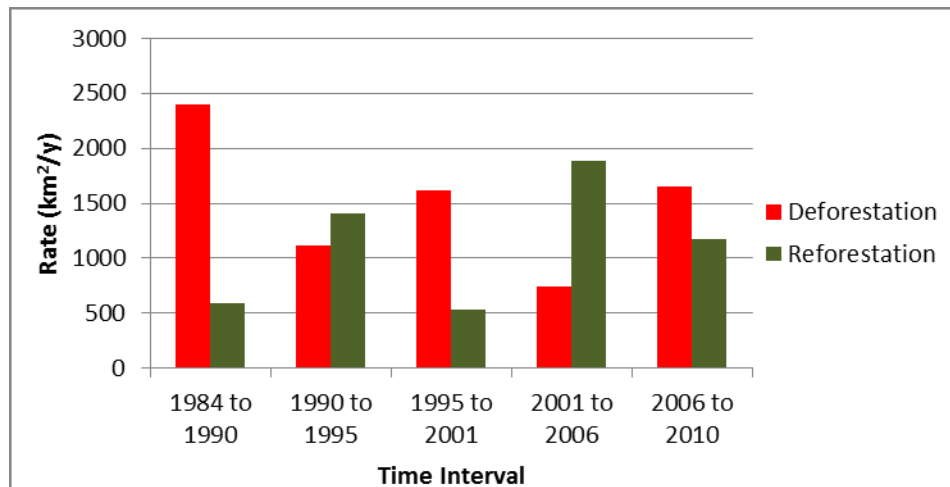


Figure 12: Deforestation and reforestation rates for entire study area at five time intervals between 1984 and 2006.

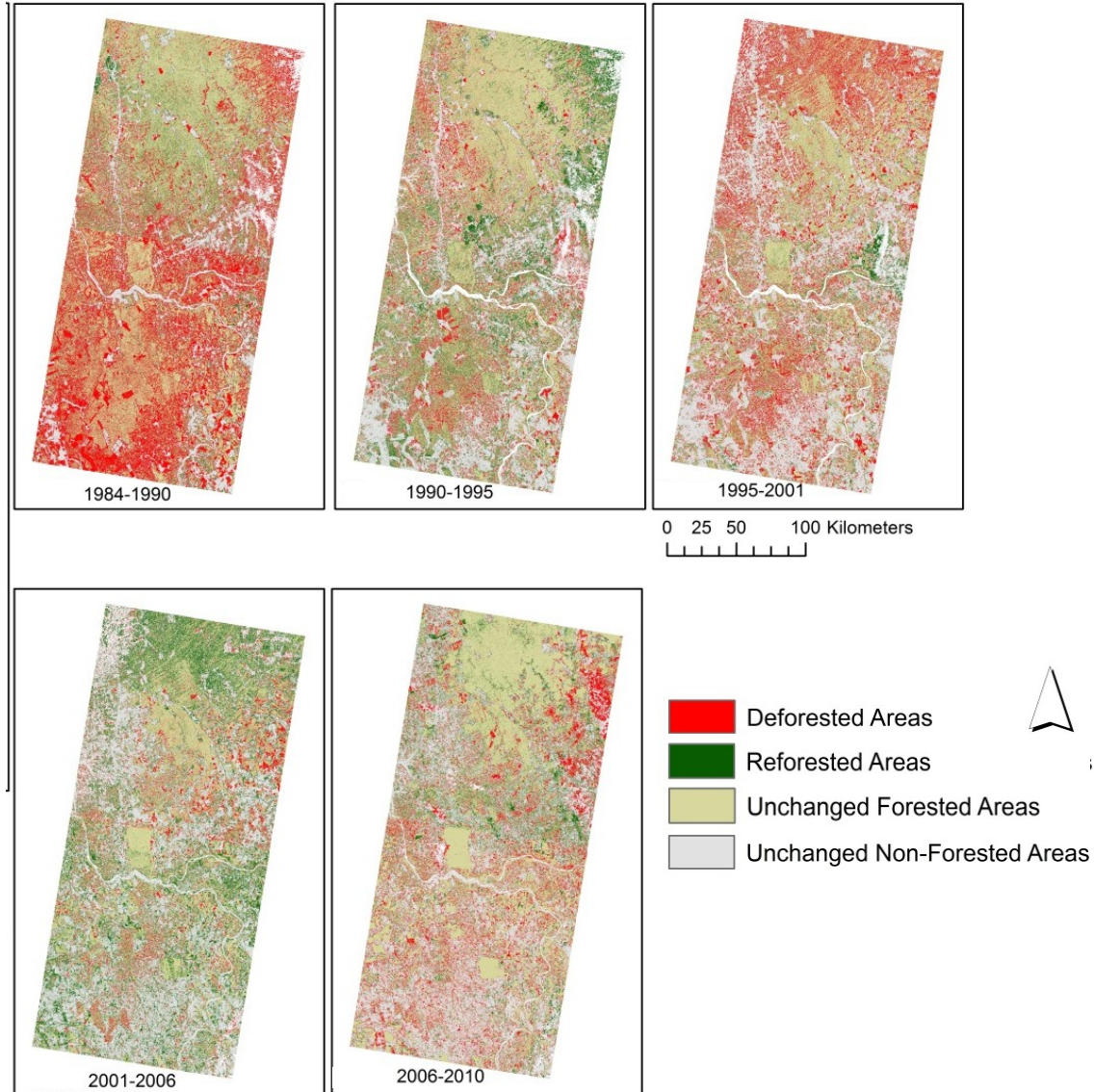


Figure 13: Percentage area of each land cover type out of the entire study area for each image.

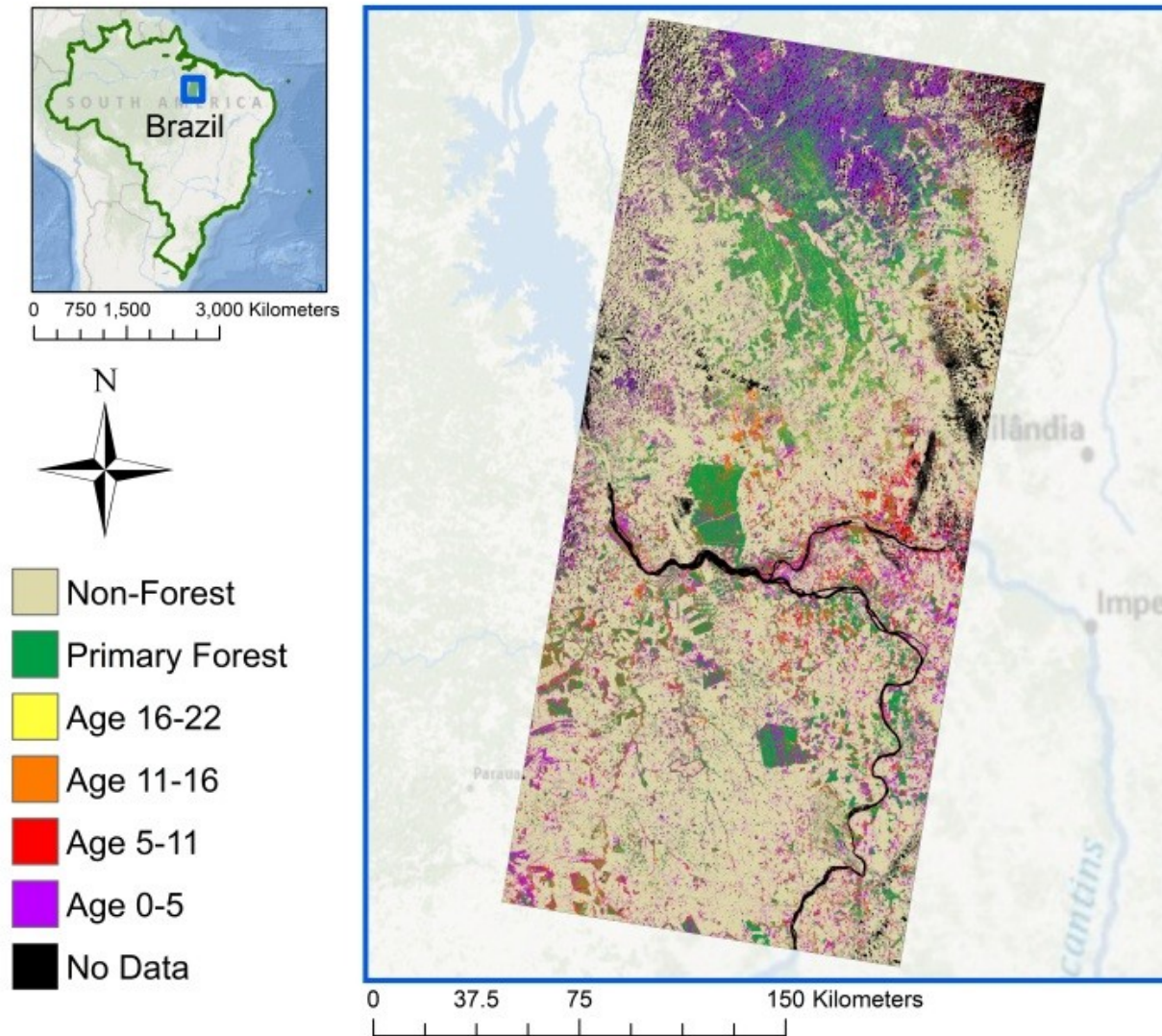


Figure 14: Secondary forest ages and primary forest derived from Landsat imagery, based on 2006 forest cover. Background: ESRI Ocean Basemap.

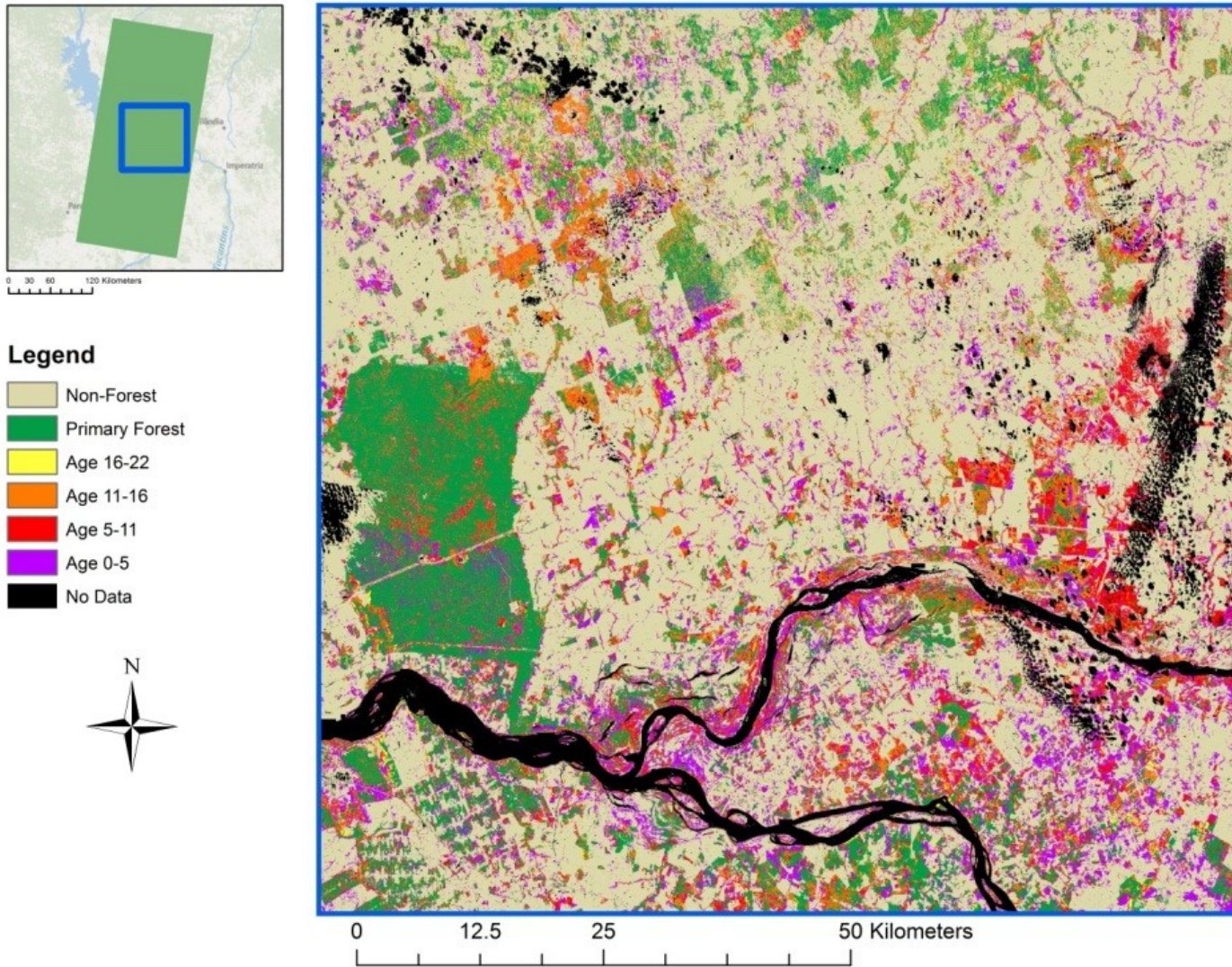


Figure 15: Close up: Secondary forest ages and primary forest derived from Landsat imagery, based on 2006 forest cover. Background: ESRI Ocean Basemap.

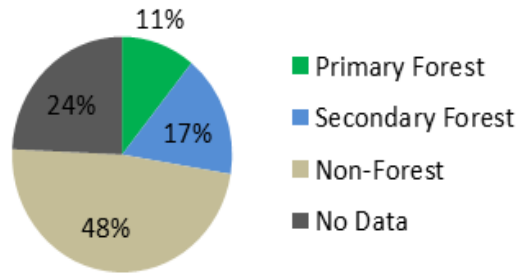


Figure 16: Percentage area of each land cover type out of the entire study area for the final age raster.

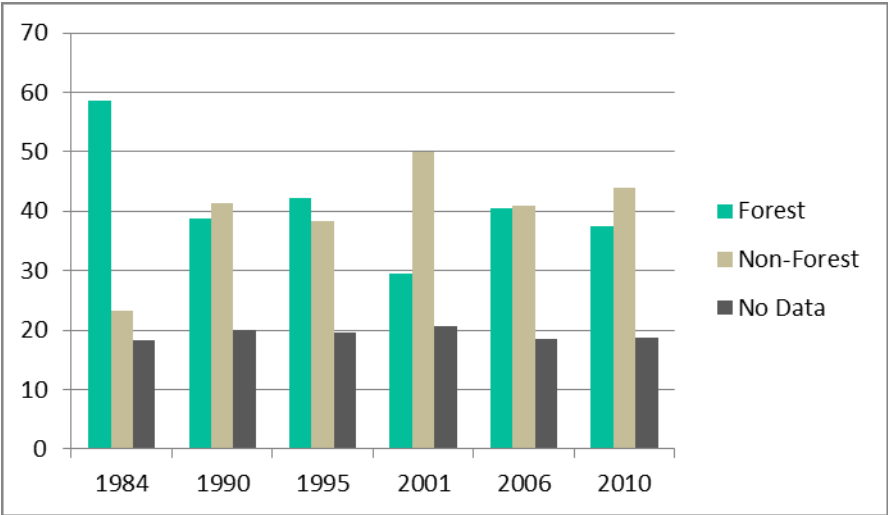


Figure 17: Percentage area of each land cover type out of the entire study area for each image.

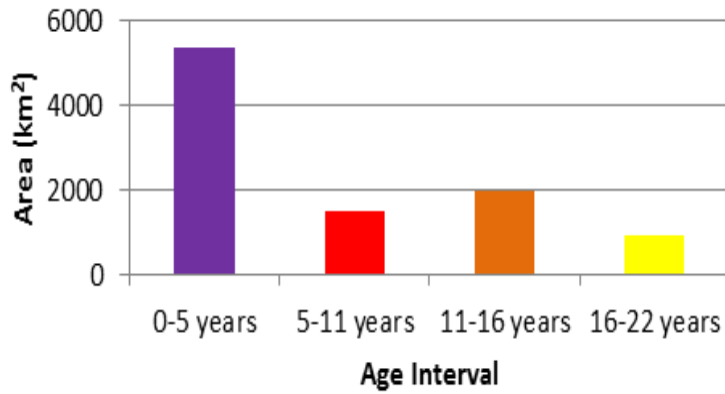


Figure 18: Area of each forest age within secondary forest in the final age raster.

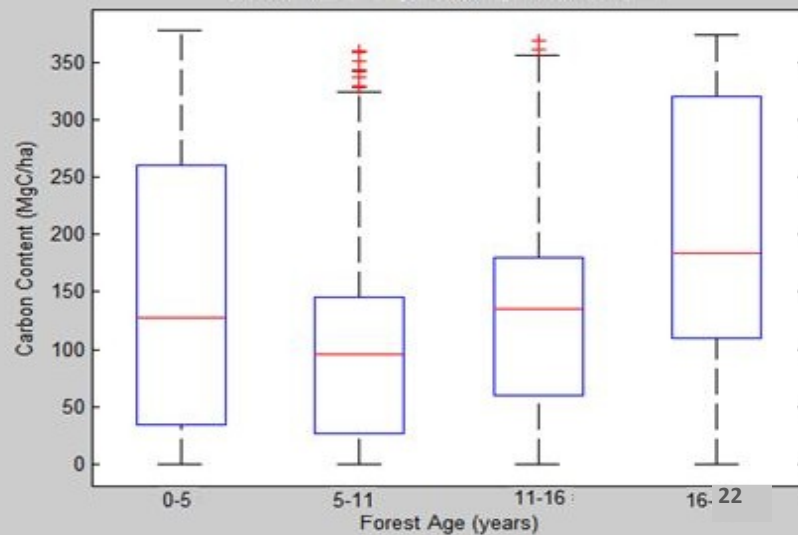


Figure 19: Carbon Content by Forest age, 1990 to 2006, based on data from 1,994 random points within secondary forest. $N_{0-5}=1085$, $N_{5-11}=294$, $N_{11-16}=428$, $N_{16-22}=187$.

Table 4: Pearson's Product-moment correlation coefficient comparing carbon to forest age for the entire study area. (r values less than 0.2 show no correlation)

Full Study Area	0.0489
-----------------	--------

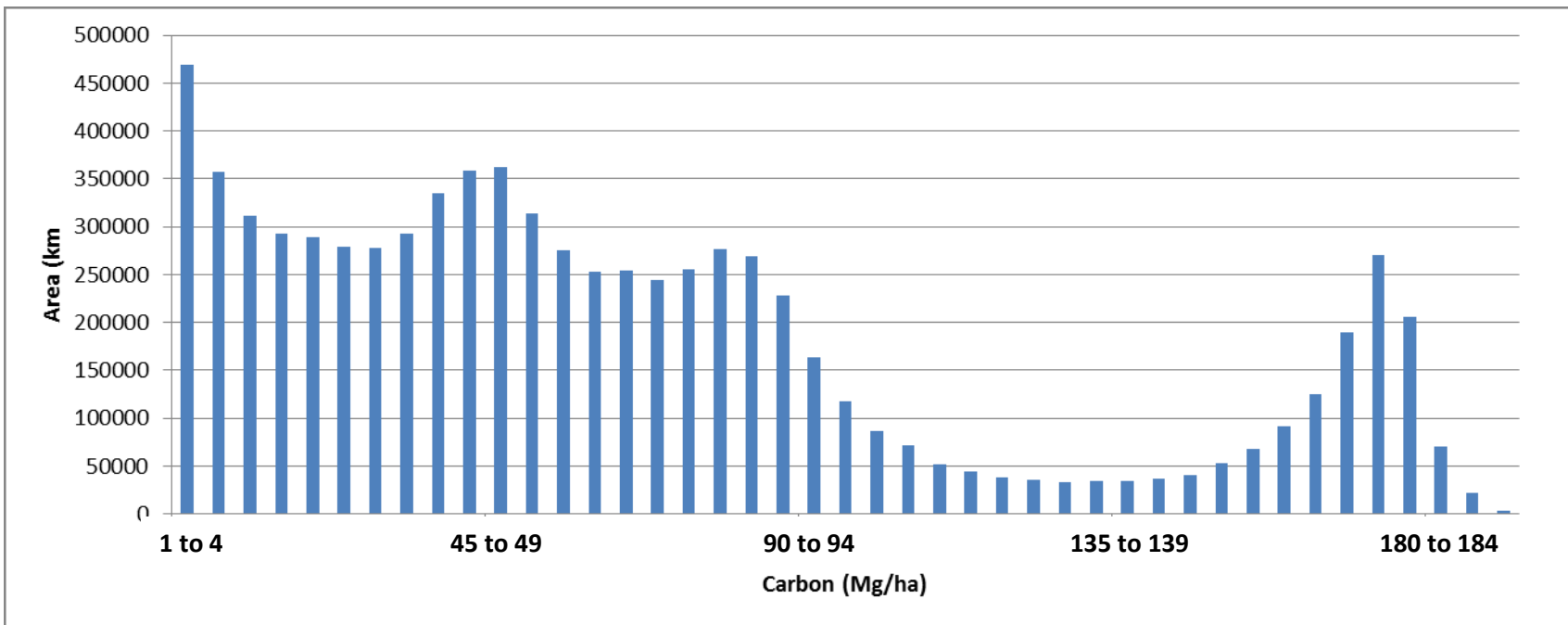


Figure 20: Histogram distribution of the carbon values within the study area for 2006. Note: all histograms have carbon values of 0 removed to improve visibility of distribution.

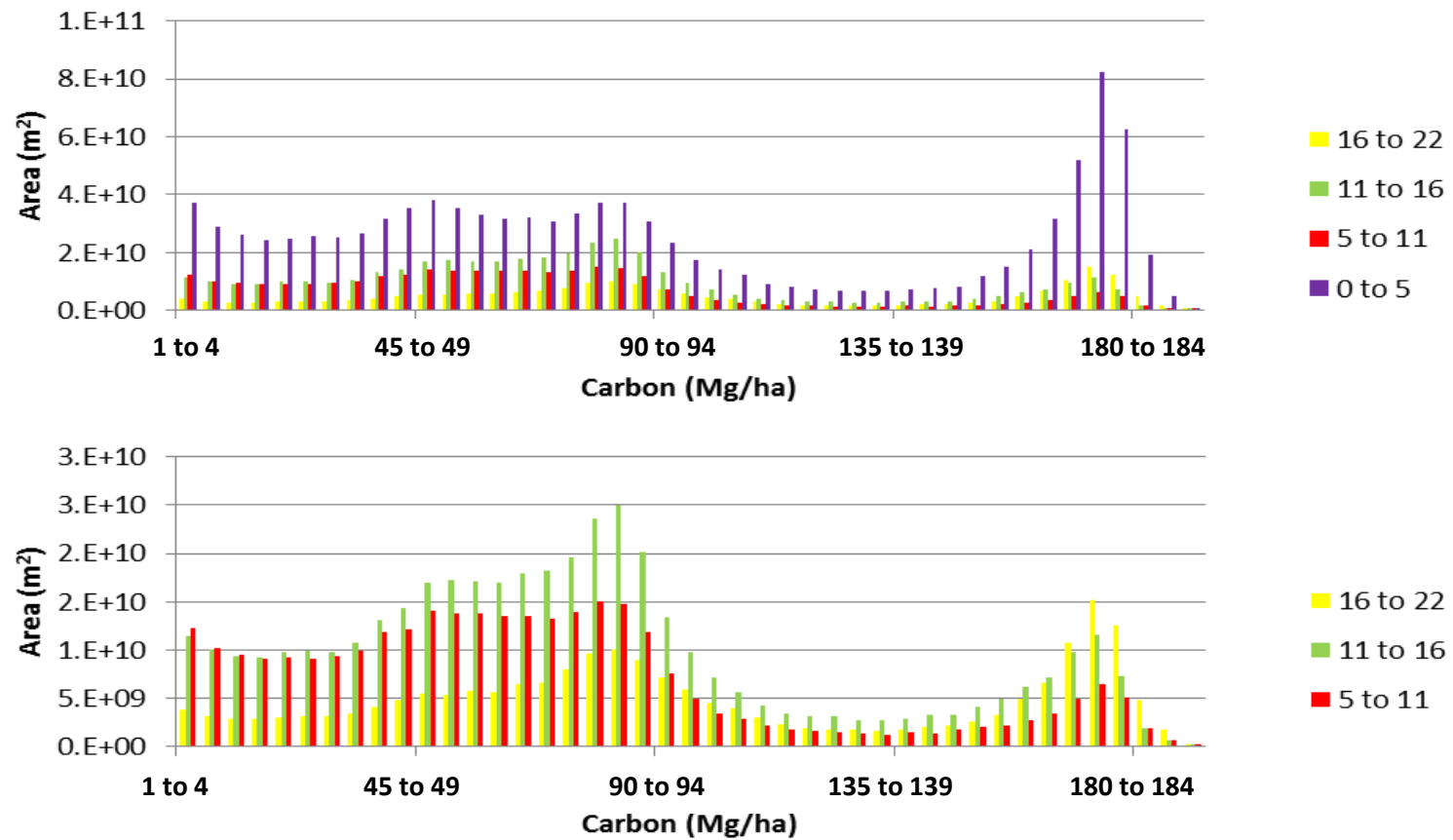


Figure 21: Histogram distributions of carbon values by age within the secondary forests in the study area. All ages represented (top) and ages greater than 5 years represented to show scale of smaller carbon values (bottom). Note that ages 11 to 16 are represented in green for contrast.

Table 5: Pearson's product-moment correlation coefficients (r) comparing each environmental variable to carbon content across the study area. p is the probability that the observed correlation is significant (p<0.05). R² is the proportion of explained variance between each relationship

Variable	p	r	Lower Bound	Upper Bound	r ²
Annual Precipitation vs Carbon in Study Area	0	0.4755	0.4408	0.5088	0.2261
Mean Annual Temperature vs Carbon in Study Area	0	0.232	0.1901	0.2731	0.0538
Latitude vs Carbon in Study Area	0	0.7017	0.6787	0.7233	0.4924
Longitude vs Carbon in Study Area	0	0.1743	0.1314	0.2166	0.0304
Elevation vs Carbon in Study Area	0.0056	-0.062	-0.1057	-0.0182	0.0038
Age vs Carbon in Study Area	0.0289	0.0489	0.005	0.0926	0.0024

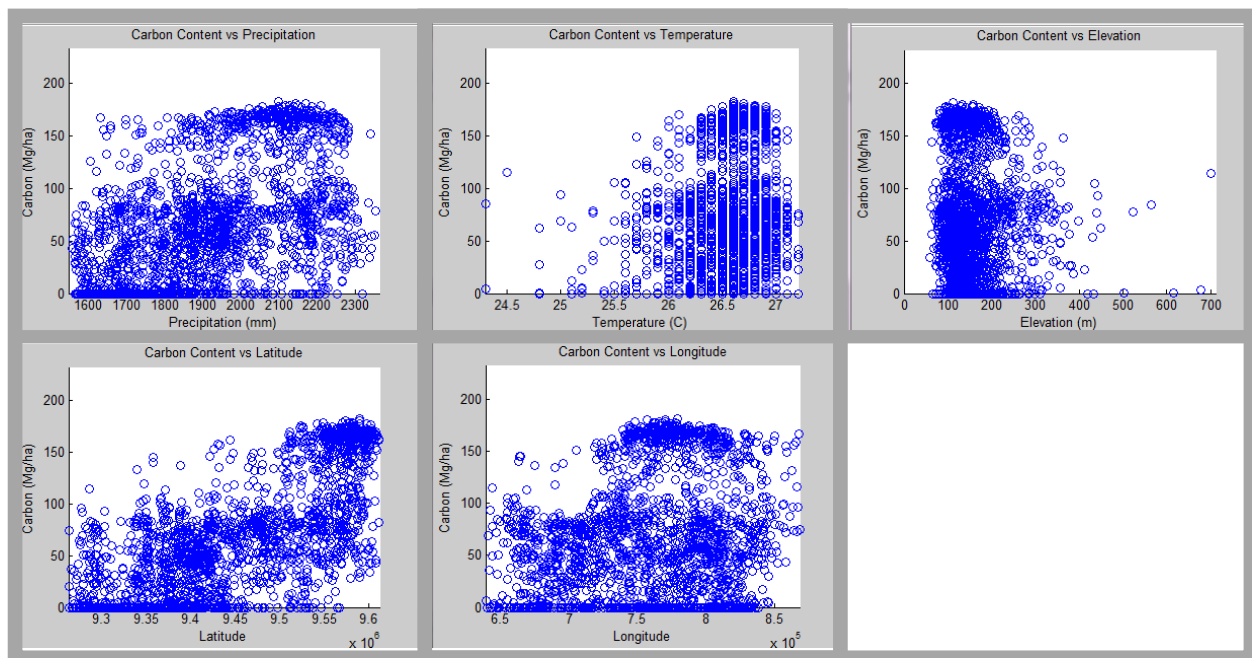


Figure 22: Carbon Content compared to other landscape variables; Clockwise from top left, Carbon vs Annual Precipitation, Carbon vs. Mean Annual Temperature, Carbon vs. Elevation, Carbon vs. Longitude, and Carbon vs. Latitude. Note lack of data between 200 and 300

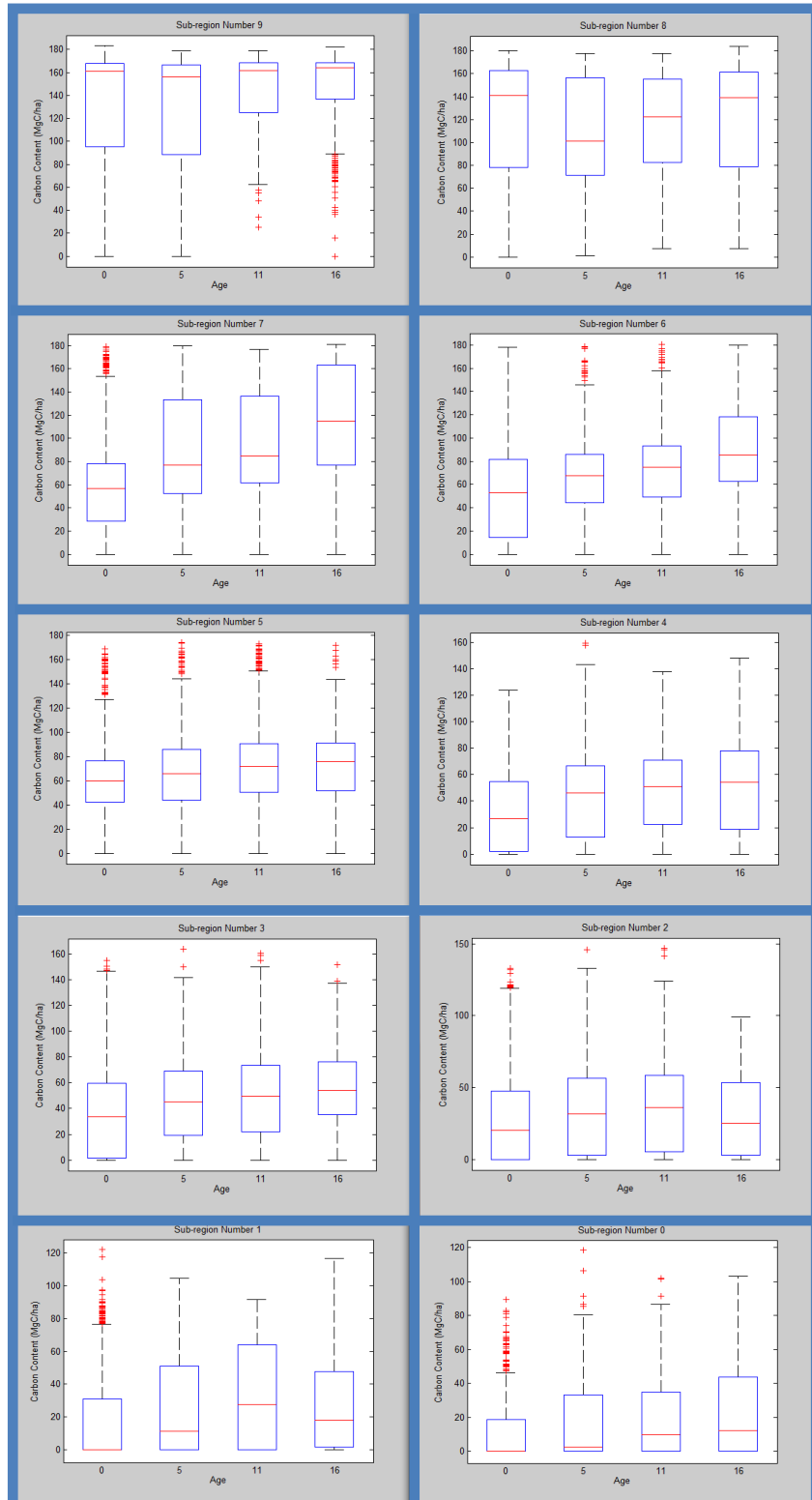


Figure 23: Boxplots: Carbon vs forest age by sub-region. Based on random points within secondary forest. See appendix for breakdown of number of points per age class for each chart.

Table 6: Sub-Regional Analysis

Sub-region Number	r	Mean Carbon (Mg/ha)	Mean Temperature (°C)	Mean Annual Precipitation (mm/y)	Mean Elevation (m)	Dominant Land Cover Type	Dominant Forest Age
0	0.1955	19	26.06	1610	186	Croplands	0-5 years
1	0.2072	18	26.12	1729	192	Croplands	0-5 years
2	0.0875	48	26.39	1734	156	Croplands	Primary
3	0.175	56	26.60	1892	142	Croplands	Primary
4	0.2246	56	26.46	1925	176	Croplands	0-5 years
5	0.1764	105	26.83	2044	128	Closed to Open Deciduous Forest	Primary
6	0.2666	111	26.21	1890	228	Closed to Open Deciduous Forest	Primary
7	0.4349	107	26.81	2195	139	Closed to Open Deciduous Forest	Primary
8	-	192	26.51	1831	160	Closed to Open Deciduous Forest	0-5 years
9	0.0806	212	26.88	2222	113	Closed to Open Deciduous Forest	0-5 years

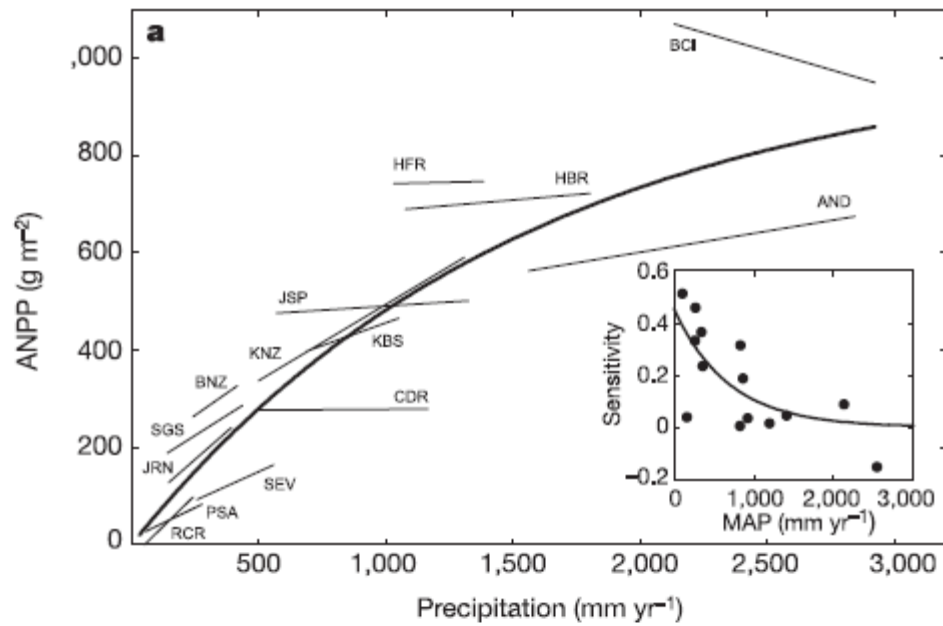


Figure 24: Linear regressions comparing Aboveground Net Primary Productivity (ANPP) vs Precipitation at 14 sites. Overall relationship across all sites shown in bold. (Huxman, et al., 2005)

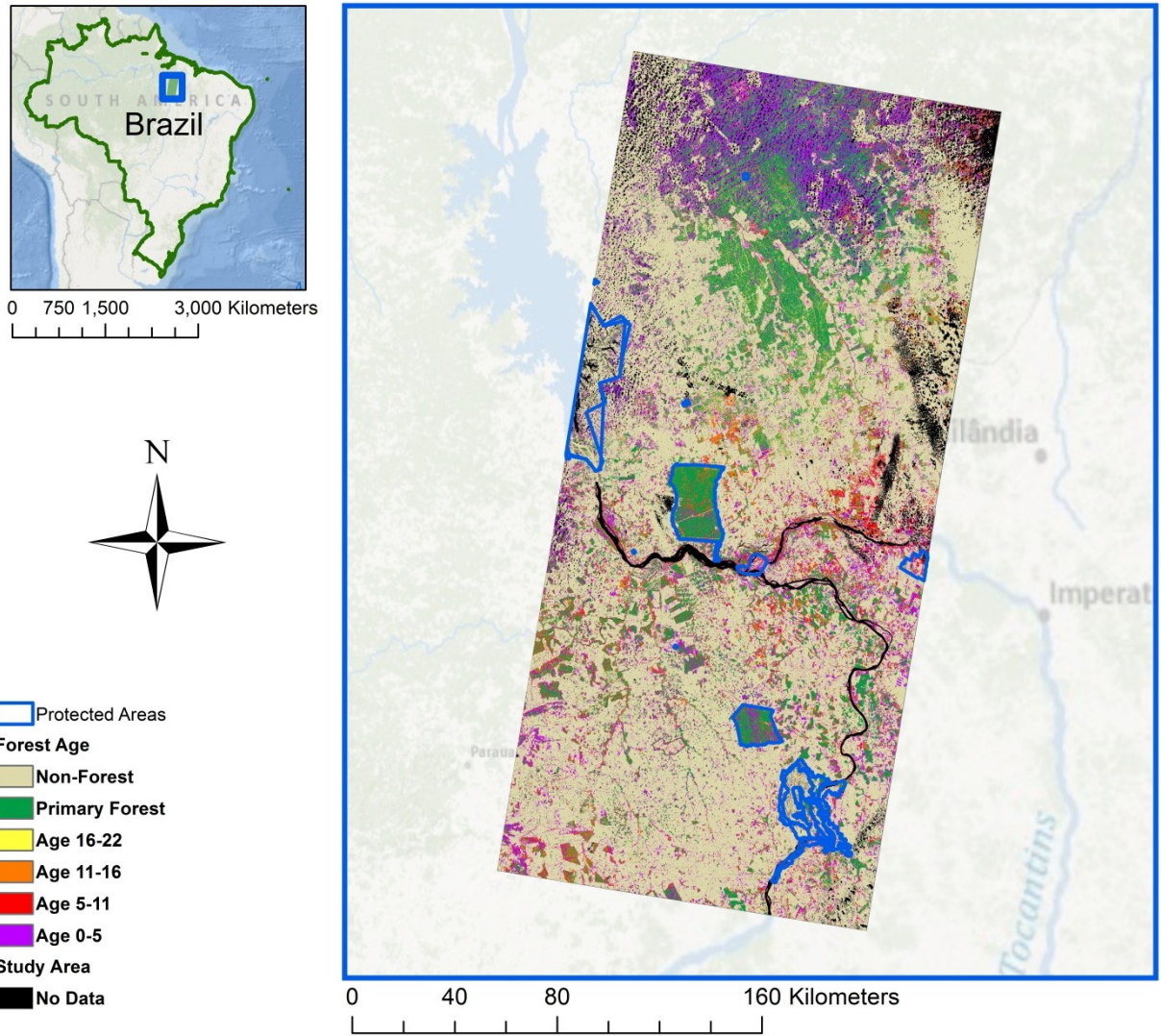


Figure 25: Protected areas and forest age. Background: ESRI Ocean Basemap.

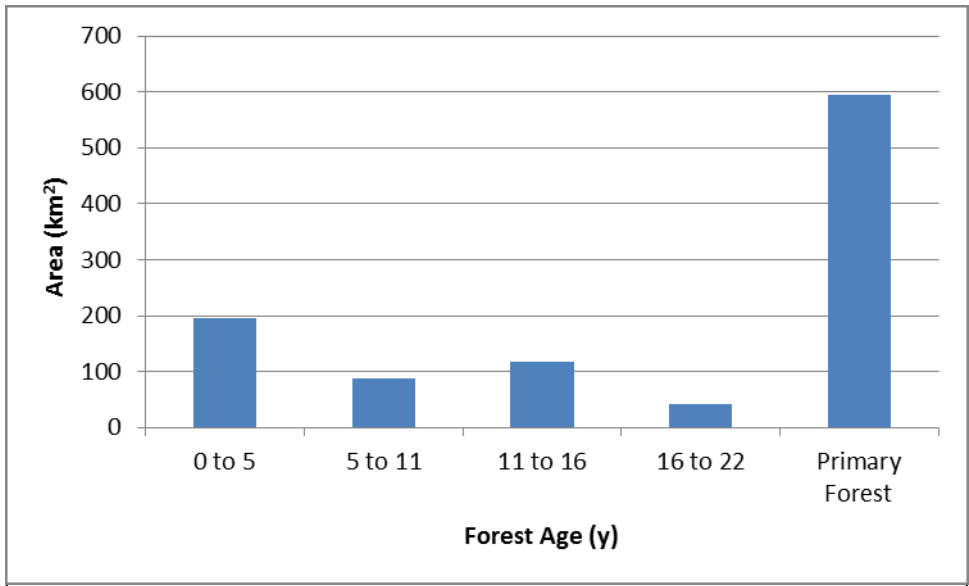


Figure 26: Forest areas within protected areas

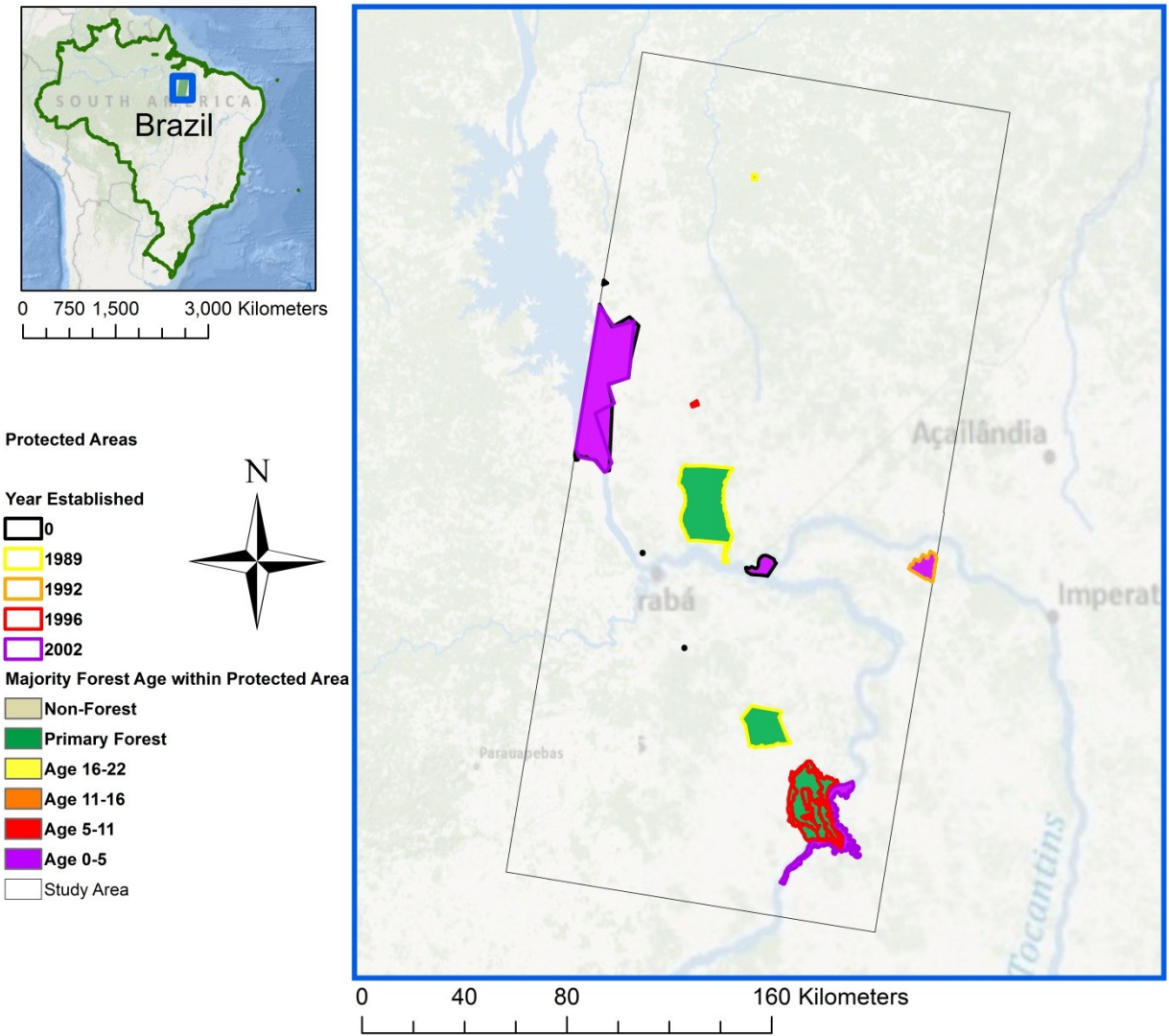


Figure 27: Majority forest age in protected study areas and establishment year for each protected area.

Table 7: Protected areas, establishment and forest age			
Name of Area	Area (km ²)	Establishment Year	Majority Forest Age
Amanay	3.10	1989	0 to 5
Múe Maria	515.07	1989	Primary
Soror	214.57	1989	Primary
Extremo Norte do Estado do Tocantins	63.49	1992	0 to 5
Lago de Santa Isabel	110.48	2002	0 to 5
Encontro das Águas	34.34	Unknown	0 to 5
Serra dos Martírios/Andorinhas	238.77	1996	Primary
Tibiria	0.90	Unknown	Primary
Fazenda Pioneira	0.89	Unknown	0 to 5
Súo Geraldo do Araguaia	157.47	Unknown	Primary
Tucuruí	600.22	Unknown	0 to 5
Nova Jacundí	2.92	1996	Primary
Lago de Tucuruí	6.69	2002	0 to 5
Súo Geraldo do Araguaia	0.05	1996	0 to 5

Sub-region Number 0

Total number of points = 1399

Forest points aged 0-5 = 742

Forest points aged 5-11 = 263

Forest points aged 11-16 = 258

Forest points aged 16-21 = 136

Correlation Coefficients

1.0000 0.1955

0.1955 1.0000

Sub-region Number 1

Total number of points = 1484

Forest points aged 0-5 = 825

Forest points aged 5-11 = 267

Forest points aged 11-16 = 353

Forest points aged 16-21 = 39

Correlation Coefficients

1.0000 0.2072

0.2072 1.0000

Sub-region Number 2

Total number of points = 2217

Forest points aged 0-5 = 1081

Forest points aged 5-11 = 439

Forest points aged 11-16 = 540

Forest points aged 16-21 = 157

Correlation Coefficients

1.0000 0.0875

0.0875 1.0000

Sub-region Number 3

Total number of points = 2092

Forest points aged 0-5 = 927

Forest points aged 5-11 = 437

Forest points aged 11-16 = 612

Forest points aged 16-21 = 116

Correlation Coefficients

1.0000 0.1750

0.1750 1.0000

Sub-region Number 4

Total number of points = 2304

Forest points aged 0-5 = 1006

Forest points aged 5-11 = 640

Forest points aged 11-16 = 519

Forest points aged 16-21 = 139

Correlation Coefficients

1.0000 0.2246

0.2246 1.0000

Sub-region Number 5

Total number of points = 2031

Forest points aged 0-5 = 912

Forest points aged 5-11 = 354

Forest points aged 11-16 = 616

Forest points aged 16-21 = 149

Correlation Coefficients

1.0000 0.1764

0.1764 1.0000

Sub-region Number 6

Total number of points = 1587

Forest points aged 0-5 = 592

Forest points aged 5-11 = 214

Forest points aged 11-16 = 383

Forest points aged 16-21 = 398

Correlation Coefficients

1.0000 0.2666

0.2666 1.0000

Sub-region Number 7

Total number of points = 1391

Forest points aged 0-5 = 716

Forest points aged 5-11 = 169

Forest points aged 11-16 = 170

Forest points aged 16-21 = 336

Correlation Coefficients

1.0000 0.4349

0.4349 1.0000

Sub-region Number 8

Total number of points = 2800

Forest points aged 0-5 = 1987

Forest points aged 5-11 = 106

Forest points aged 11-16 = 522

Forest points aged 16-21 = 185

Correlation Coefficients

1.0000 -0.0158

-0.0158 1.0000

Sub-region Number 9

Total number of points = 3028

Forest points aged 0-5 = 2325

Forest points aged 5-11 = 188

Forest points aged 11-16 = 196

Forest points aged 16-21 = 319

Correlation Coefficients

1.0000 0.0806

0.0806 1.0000